Applicability of hydrodynamics in large and small systems

Victor E. Ambruș

Physics Faculty, West University of Timișoara, Romania

Work in collaboration with C. Werthmann (Wrocław) and S. Schlichting (Bielefeld)

PRD **107** (2023) 094013 (arXiv:2211.14379)
PRL **130** (2023) 152301 (arXiv:2211.14356)

QCD challenges from pp to AA collisions, 5$^{\rm th}$ Edition
04/09/2024

Universitatea de Vest din Timişoara

Outline

Introduction

Transport models

Pre-equilibrium: Bjorken attractor

Scaled hydro

Hybrid simulations

Conclusions

QGP in the laboratory

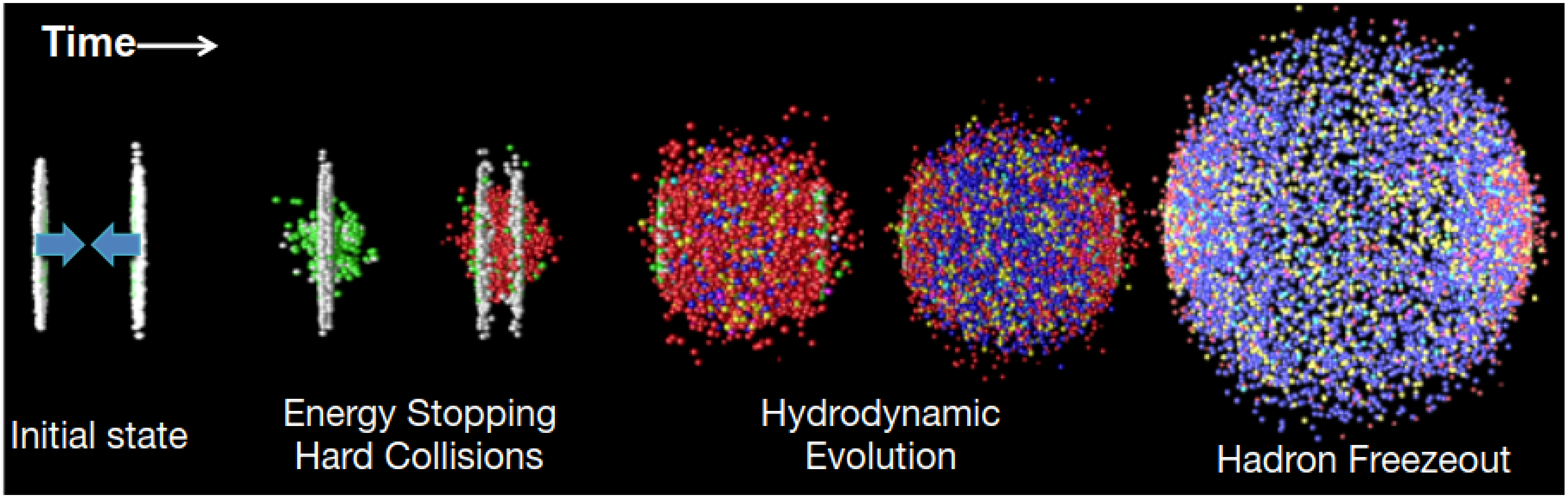

- Bjorken coordinates:
  $\tau = \sqrt{t^2 - z^2}$;
  $\eta = \tanh^{-1}(z/t)$.
- Ultra-relatistic heavy-ion collisions ($\sqrt{s_{NN}} = 5.02$ TeV PbPb) deposit $dE_\perp/d\eta \sim 1280$ GeV.
- Due to rapid longitudinal expansion, the QGP cools, reaching $k_B T \sim 350$ MeV at $\tau \simeq 1$ fm$/c$.

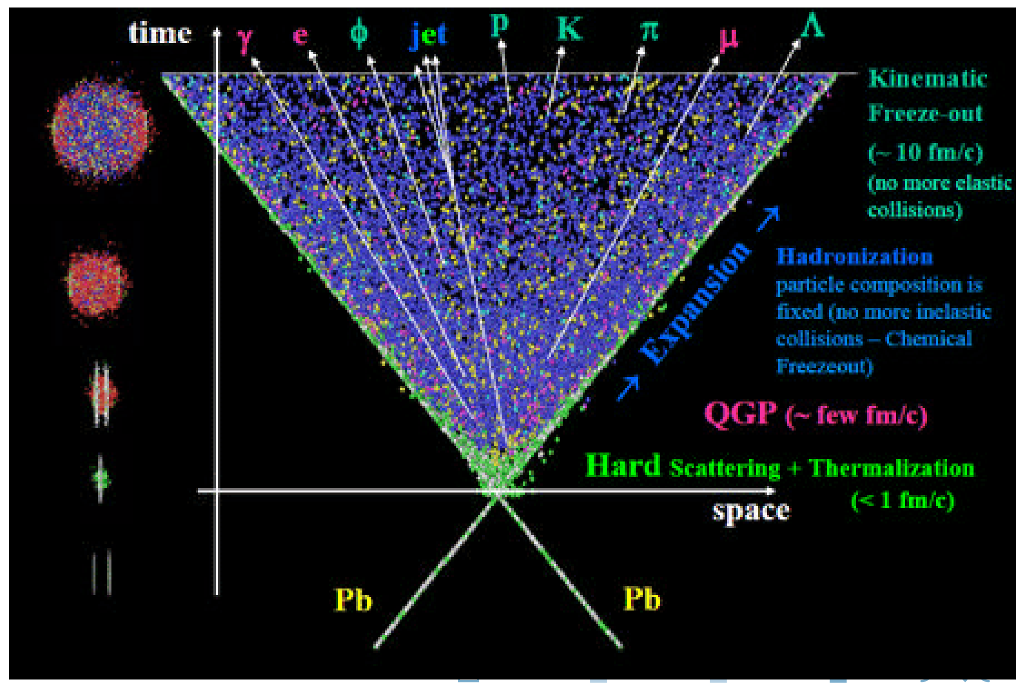

[Venaruzzo, PhD Thesis, 2011]

Bjorken model

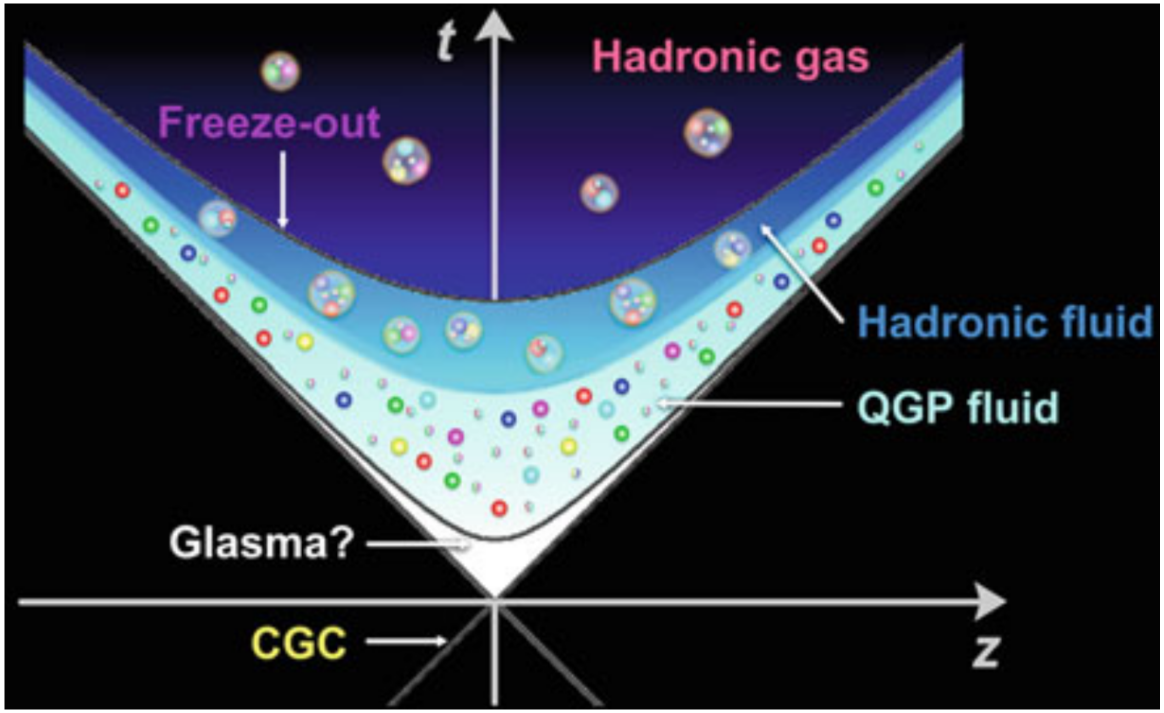

[A. Monnai, PhD Thesis (Tokyo, 2014)]

Nuclear collision model:

- Initial state: Colour glass condensate
- Early stage: Glasma?
- Onset of QGP
- Hadronisation
- Freeze-out

Hadronic Collisions in Experiment

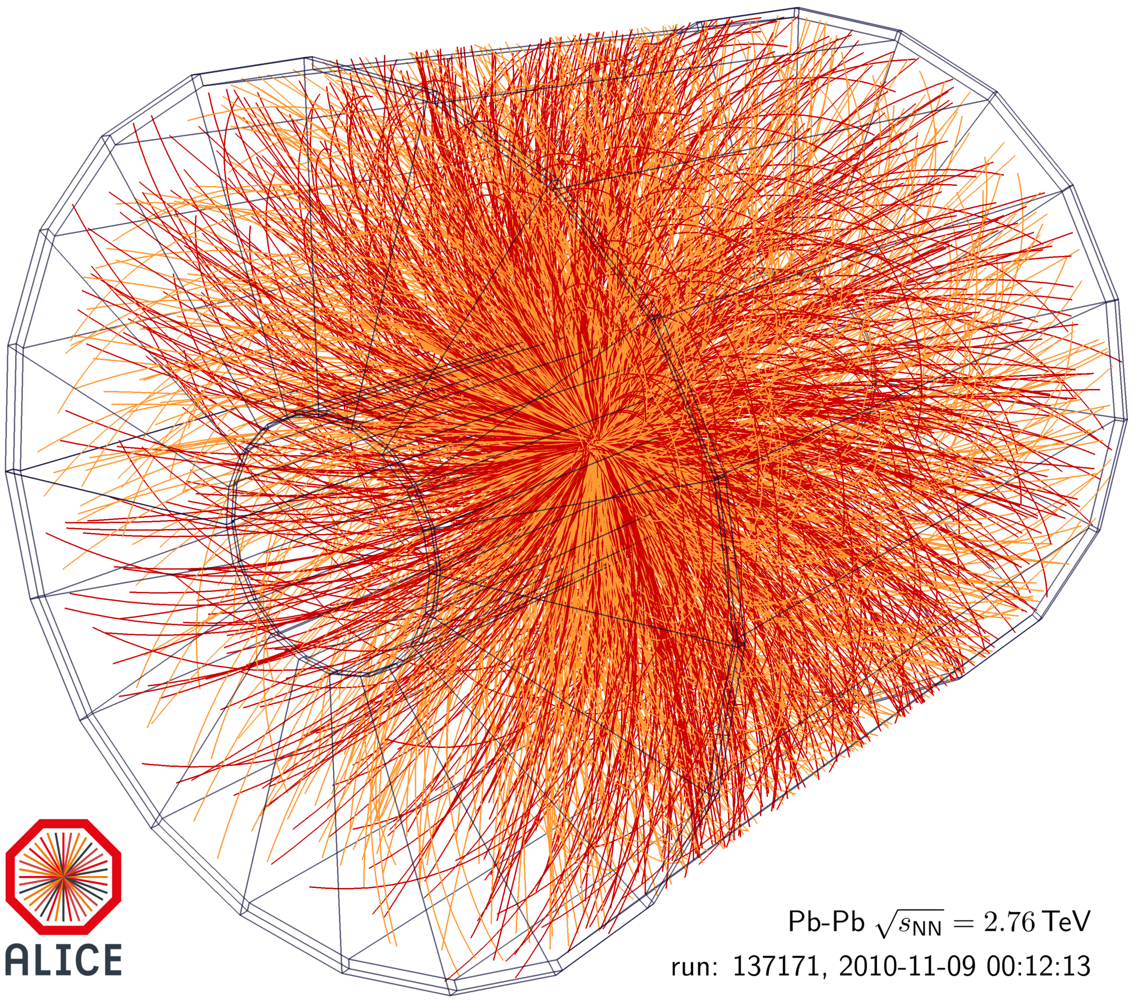

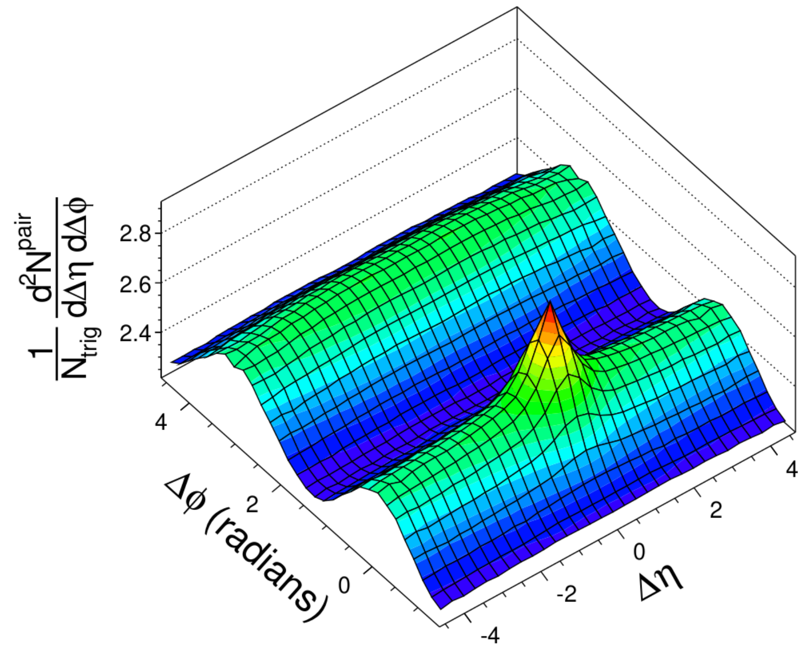

Figure (cropped): CMS Collaboration PLB 724 (2013) 213;

PbPb $\sqrt{s_{\rm NN}} = 2.76$ TeV

- Correlation peak at $(\Delta\phi, \Delta\eta) = (0, 0)$ due to jet fragmentation.
- Bands at $\Delta\phi = 0$ (near-side) and π (away-side) are due to elliptic flow, $\sim \cos(2\Delta\phi)$.

Transverse plane observables

- The overlap region between the colliding nuclei also expands in the transverse plane.
- The strong coupling of the QGP leads to hydrodynamic-like behaviour.
- Initial eccentricities ϵ_n lead to momentum-space anisotropies, characterized by flow harmonics v_n.
- $v_2 \equiv$ elliptic flow was one of the first exp. signatures for the formation of the QGP medium.

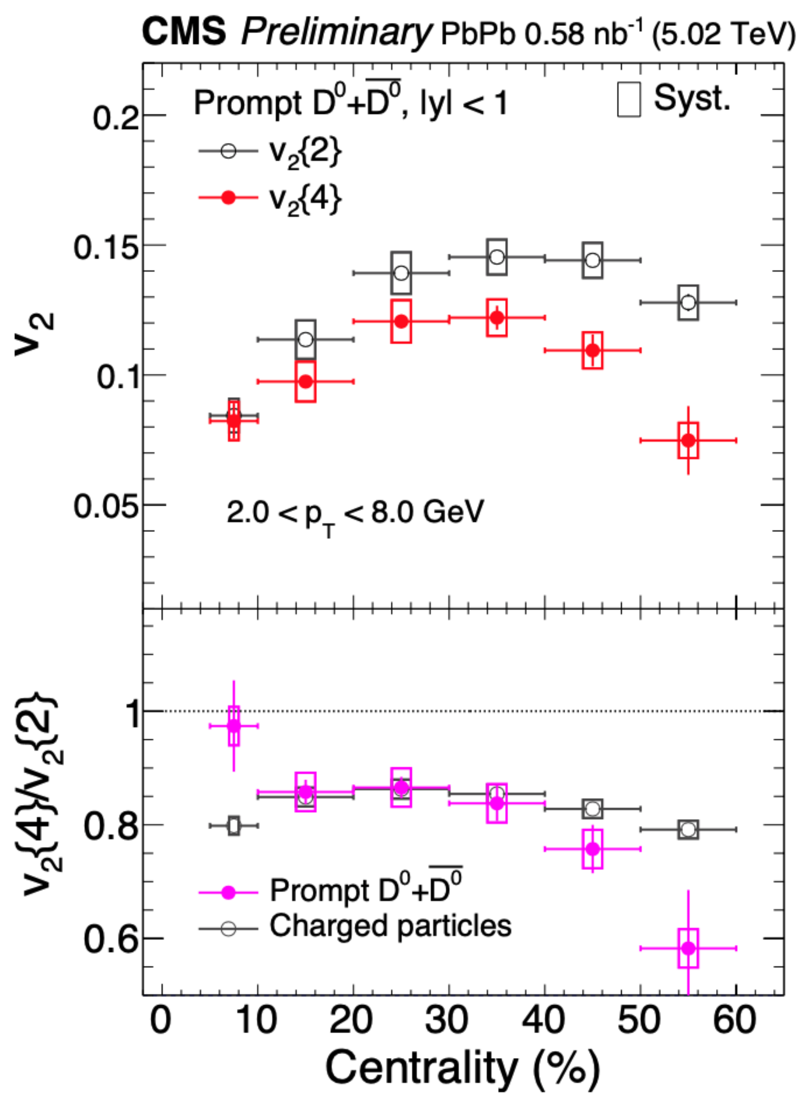

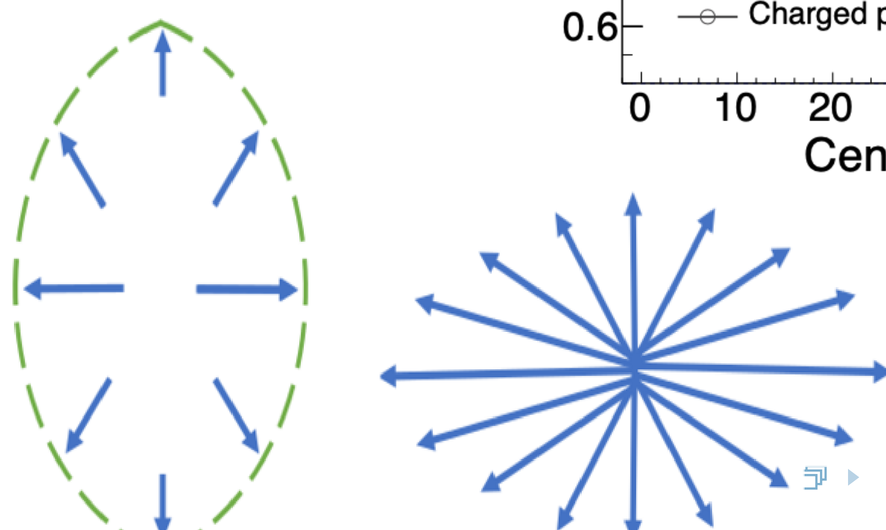

Standard modelling of heavy ion collisions

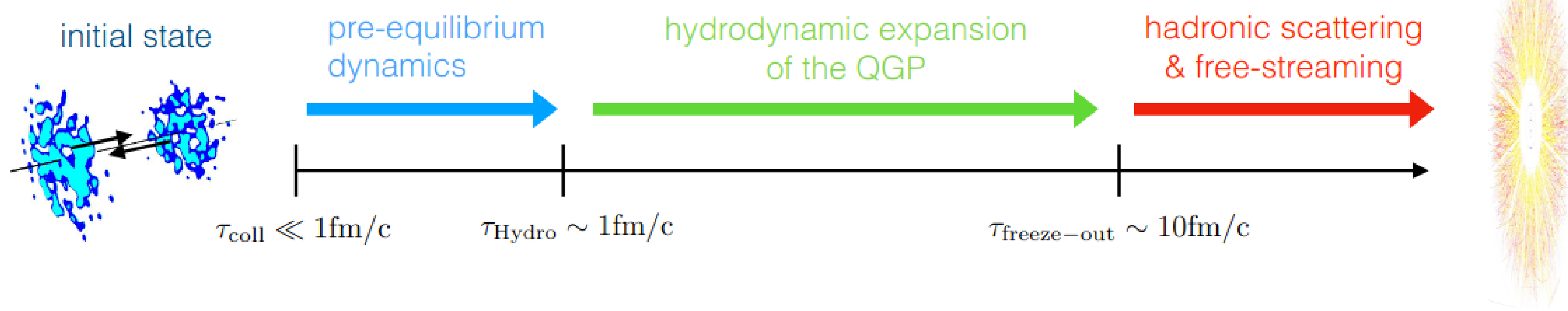

- Shortly after the collision, the system is in a far-from-equilibrium state.
- Pre-equilibrium dynamics require a non-equilibrium description.
- Strongly-interacting QGP leaves imprints of thermalization and collectivity in final-state observables:

  v_n, $\langle p_T \rangle$, particle yields, ...
- Large systems $(A + A)$ equilibrate quickly and hydrodynamics becomes applicable.
- For small systems $(p + A,\ p + p)$, a similar argument ~~undisputedly holds~~ is hard to digest...

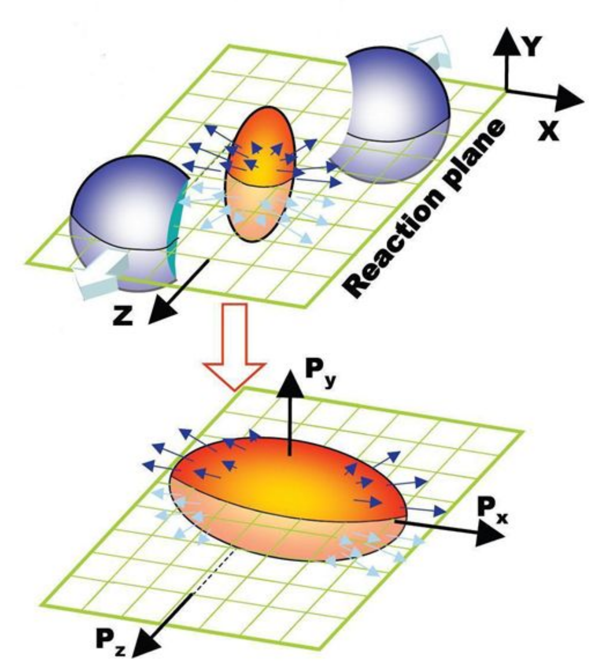

Hiroshi Masui (2008)

Small systems

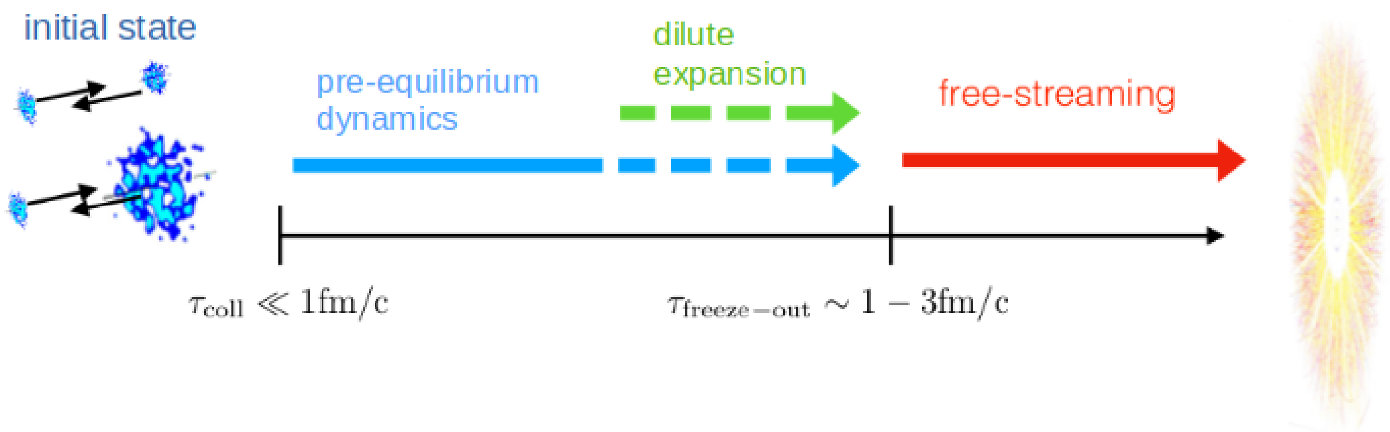

Very dilute, hydrodynamics not necessarily applicable

- still collective behaviour is observed!

  Nagle, Zajc Ann.Rev.Nucl.Part. 68 (2018) 211

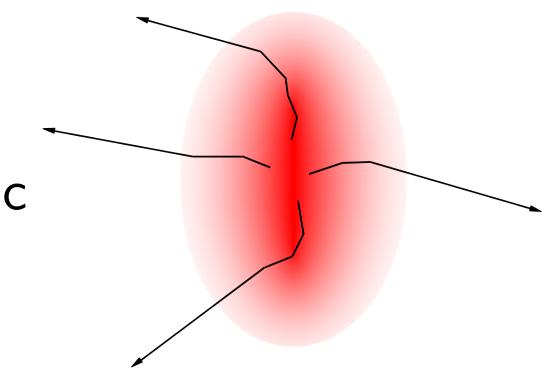

Collectivity can also be explained in kinetic theory, a mesoscopic description which does not rely on equilibration.

- KT interpolates between free streaming at small opacities and hydrodynamics at large opacities!

Aim

Benchmarking of hydro for transverse flow observables w.r.t. kinetic theory for a simplified (conformal) fluid on full range from small to large system sizes.

Eccentricities and harmonic response

Transverse plane profiles with $\cos(n\varphi)$ eccentricities:

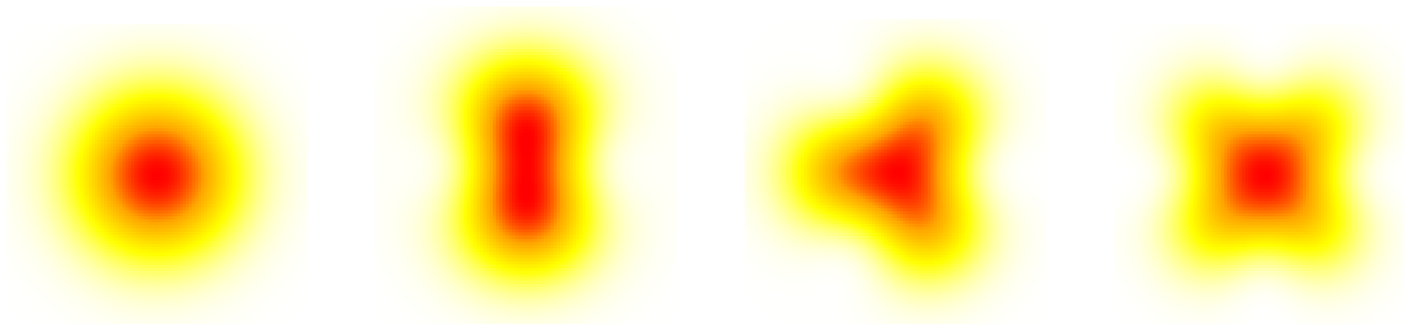

(no ecc.) $(n = 2)$ $(n = 3)$ $(n = 4)$

Inhomogeneous transverse gradients $\Rightarrow$ inhomogeneous flow:

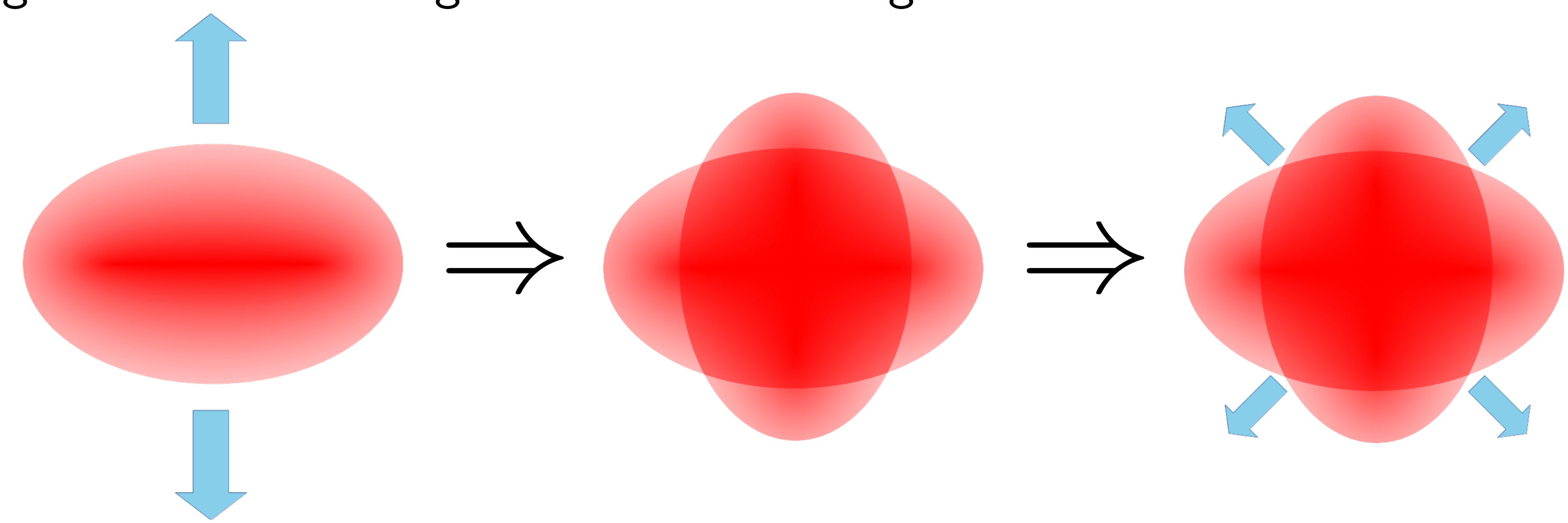

KT: Model and setup

- Mesoscopic description in terms of averaged on-shell phase-space distribution:

$$f(\tau, \mathbf{x}_\perp, \eta, \mathbf{p}_\perp, y) = \frac{(2\pi)^3}{\nu_{\rm eff}} \frac{{\rm d}N}{{\rm d}^3x\,{\rm d}^3p}(\tau, \mathbf{x}_\perp, \eta, \mathbf{p}_\perp, y),$$

  describing massless bosons with $\nu_{\rm eff} = 2(N_c^2 - 1) + \frac{7}{8} \times 4N_c N_f \to 42.25$
- Time evolution is described via the Boltzmann eq. in conformal RTA:

$$p^\mu \partial_\mu f = C_{\rm RTA}[f] = -\frac{p^\mu u_\mu}{\tau_R}(f - f_{\rm eq}), \quad f_{\rm eq} = \frac{1}{e^{p^\mu u_\mu / T} - 1}.$$

- We take $\eta/s = \text{const}$, while τ_R is related to η/s via

$$\tau_R = \frac{5\eta}{sT}. \tag{1}$$

- We assume boost invariance $\Rightarrow$ f depends only on $y - \eta$.
- Parametrizing $f \equiv f(\tau, \mathbf{x}_\perp; \mathbf{p}_\perp, v^z)$, with $v_z = \tanh(y - \eta_s) = \tau p^\eta / p^\tau$, we have

$$\frac{\partial f}{\partial \tau} + \mathbf{v}_\perp \cdot \boldsymbol{\nabla}_\perp f - \frac{v^z}{\tau}(1 - v_z^2)\frac{\partial f}{\partial v^z} = -\frac{1}{\tau_R}(f - f_{\rm eq}). \tag{2}$$

KT: Initial state

- At τ_0, we take

$$f(\tau_0, \mathbf{x}_\perp; \mathbf{p}_\perp, v^z) = \frac{(2\pi)^3}{\nu_{\text{eff}}} \frac{\delta(v^z)}{\tau_0 p_\perp} \frac{dN_0}{d^2\mathbf{x}_\perp d^2\mathbf{p}_\perp d\eta}. \tag{3}$$

- We further assume $f(\tau_0)$ depends only on $|\mathbf{p}_\perp|$ (no transverse anisotropies) and

$$\frac{dN_0}{d^2\mathbf{x}_\perp d^2\mathbf{p}_\perp d\eta} = F\left(\frac{Q_s(\mathbf{x}_\perp)}{p_\perp}\right), \tag{4}$$

  where F is some function of the ratio of the momentum scale $Q_s(\mathbf{x}_\perp)$ and $p_\perp$ satisfying

$$\epsilon(\tau_0, \mathbf{x}_\perp) = \frac{1}{\tau_0} \int d^2\mathbf{p}_\perp p_\perp \frac{dN_0}{d^2\mathbf{x}_\perp d^2\mathbf{p}_\perp dy}. \tag{5}$$

- $T^{\mu\nu} = \int_\mathbf{p} p^\mu p^\nu f$ is initialized as [$\int_\mathbf{p} \equiv \frac{\nu_{\text{eff}}}{(2\pi)^3}\sqrt{-g}\int d^3p/p^\tau$]

$$T_0^{\mu\nu} = \epsilon_0(\mathbf{x}_\perp) \times \text{diag}(1, 1/2, 1/2, 0),$$

  i.e. the longitudinal pressure vanishes, $P_L(\tau_0) = 0$.

- $\Rightarrow$ system evolution depends only on $\epsilon_0(\mathbf{x}_\perp)$ and **opacity** $\hat{\gamma}$.

System opacity $\hat{\gamma}$

- The system evolution depends only on the opacity $\sim$ "total interaction rate"

Kurkela, Wiedemann, Wu EPJC 79 (2019) 965

$$\hat{\gamma} = \left(5\frac{\eta}{s}\right)^{-1}\left(\frac{1}{a\pi}R\frac{\mathrm{d}E_\perp^{(0)}}{\mathrm{d}\eta}\right)^{1/4}, \qquad a = \frac{\pi^2}{30}\nu_{\rm eff}.$$

  - $\hat{\gamma}$ encodes dependencies on viscosity , transverse size and energy scale, with

$$\frac{\mathrm{d}E_\perp^{(0)}}{\mathrm{d}\eta} = \int_{\mathbf{x}_\perp}\tau_0\epsilon_0, \qquad R^2\frac{\mathrm{d}E_\perp^{(0)}}{\mathrm{d}\eta} = \int_{\mathbf{x}_\perp}\tau_0\epsilon_0\mathbf{x}_\perp^2.$$

- We take as initial condition the $30-40\%$ centrality-class average of Pb+Pb at 5.02 TeV $\Rightarrow R \simeq 2.78$ fm and $\mathrm{d}E_\perp^{(0)}/\mathrm{d}\eta = 1280$ GeV

Borghini, Borrell, Feld, Roch, Schlichting, Werthmann PRC 107 (2023), 034905

  - For a fixed initial profile, $\hat{\gamma}$ can be varied via η/s:

$$\hat{\gamma} \approx \frac{11}{4\pi\eta/s}.$$

30-40%

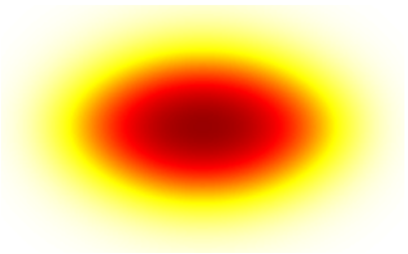

Hydro setup

- In hydro, the system is described directly by the energy-momentum tensor,

$$T^{\mu\nu} = \epsilon u^\mu u^\nu - P\Delta^{\mu\nu} + \pi^{\mu\nu}, \qquad \Delta^{\mu\nu} = g^{\mu\nu} - u^\mu u^\nu.$$

- Energy-momentum conservation $\partial_\mu T^{\mu\nu} = 0$ entails

$$\dot\epsilon + (\epsilon + P)\theta - \pi^{\mu\nu}\sigma_{\mu\nu} = 0,$$
$$(\epsilon + P)\dot u^\mu - \nabla^\mu P + \Delta^\mu{}_\lambda \partial_\nu \pi^{\lambda\nu} = 0,$$

  where $\theta = \partial_\mu u^\mu$ and $\sigma_{\mu\nu} = \nabla_{\langle\mu} u_{\nu\rangle}$,[1] with $\nabla_\mu \equiv \Delta^\alpha_\mu \partial_\alpha$.
- In MIS viscous hydro, $\pi^{\mu\nu}$ evolves according to

$$\tau_\pi \dot\pi^{\langle\mu\nu\rangle} + \pi^{\mu\nu} = 2\eta\sigma^{\mu\nu} + 2\tau_\pi \pi^{\langle\mu}_\lambda \omega^{\nu\rangle\lambda} - \delta_{\pi\pi}\pi^{\mu\nu}\theta - \tau_{\pi\pi}\pi^{\lambda\langle\mu}\sigma^{\nu\rangle}_\lambda + \phi_7 \pi^{\langle\mu}_\alpha \pi^{\nu\rangle\alpha},$$

  where $\omega_{\mu\nu} = \frac{1}{2}[\nabla_\mu u_\nu - \nabla_\nu u_\mu]$ is the vorticity tensor.
- The transport coefficients are chosen for compatibility with RTA:

[Ambruș, Molnár, Rischke, PRD **106** (2022) 076005]

$$\eta = \frac{4}{5}\tau_\pi P, \quad \delta_{\pi\pi} = \frac{4\tau_\pi}{3}, \quad \tau_{\pi\pi} = \frac{10\tau_\pi}{7}, \quad \phi_7 = 0, \quad \tau_\pi = \tau_R.$$

- Numerical solution obtained using **vHLLE**. [Karpenko, Huovinen, Bleicher, CPC 185 (2014) 3016]

[1] $A^{\langle\mu\nu\rangle} = \Delta^{\mu\nu}_{\alpha\beta} A^{\alpha\beta}$, $\Delta^{\mu\nu}_{\alpha\beta} = \frac{1}{2}(\Delta^\mu_\alpha \Delta^\nu_\beta + \Delta^\mu_\alpha \Delta^\nu_\beta) - \frac{1}{3}\Delta^{\mu\nu}\Delta_{\alpha\beta}$.

$0+1$-D conformal Bjorken flow

- At early times ($\tau \ll R$), transverse dynamics are irrelevant and

$$T^{\mu}{}_{\nu} = \mathrm{diag}(e, -\mathcal{P}_T, -\mathcal{P}_T, -\mathcal{P}_L),$$
$$\pi^{\mu}{}_{\nu} = \pi_d \times \mathrm{diag}\left(0, \tfrac{1}{2}, \tfrac{1}{2}, -1\right), \tag{6}$$

  such that $\mathcal{P}_T = P - \frac{1}{2}\pi_d$ and $\mathcal{P}_L = P + \pi_d$.

- Under MIS hydro, ϵ and π_d evolve according to

$$\tau \frac{\partial \epsilon}{\partial \tau} + \epsilon + \mathcal{P}_L = 0, \qquad \tau \frac{\partial \pi_d}{\partial \tau} + \left(\lambda + \frac{\tau}{\tau_R}\right)\pi_d + \frac{4\eta}{3\tau_R} = 0, \tag{7}$$

  where $\lambda = (\delta_{\pi\pi} + \frac{1}{3}\tau_{\pi\pi})/\tau_\pi = 38/21$ for compatibility with RTA.

- It is convenient to employ the conformal scaling parameter

$$\tilde{w} = \frac{5\tau}{4\pi\tau_R} = \frac{\tau T}{4\pi\eta/s} \qquad \Rightarrow \qquad \tau \frac{d\tilde{w}}{d\tau} = \tilde{w}\left(\frac{2}{3} - f_\pi\right). \tag{8}$$

- Then, the function $f_\pi = \pi_d/\epsilon$ obeys a closed-form differential equation:

$$\tilde{w}\left(\frac{2}{3} - \frac{f_\pi}{4}\right)\frac{df_\pi}{d\tilde{w}} + \left(\lambda - \frac{4}{3} + \frac{4\pi\tilde{w}}{5} - f_\pi\right) f_\pi + \frac{16}{45} = 0, \tag{9}$$

  showing that $f_\pi \equiv f_\pi(\tilde{w})$.

Attractor solution

- Free-streaming fixed point (around $\tilde{w} = 0$):

$$f_\pi(\tilde{w} \ll 1) = f_{\pi;0} + f_{\pi;1}\tilde{w} + \dots \tag{10}$$

- $f_{\pi;0}$ and $f_{\pi;1}$ are independent on ICs, but depend on the theory:

$$f_{\pi;0}^{\text{Hydro}} \simeq -0.4, \qquad f_{\pi;0}^{\text{RKT}} = \frac{1}{3}. \tag{11}$$

- The value of $f_{\pi;0}$ influences $\mathcal{P}_L/\mathcal{P}_T$ at early time:

$$\frac{\mathcal{P}_L}{\mathcal{P}_T} = \frac{1+3f_\pi}{1-\frac{3}{2}f_\pi} \xrightarrow[\tilde{w}\to 0]{} \begin{cases} -0.13, & \text{Hydro}, \\ 0, & \text{RKT}. \end{cases} \tag{12}$$

- Hydro fixed point (around $\tilde{w}^{-1} = 0$)

$$f_\pi(\tilde{w} \gg 1) = -\frac{4}{9\pi\tilde{w}}, \tag{13}$$

which is independent of ICs and of theory.

Hydro vs Kinetic theory

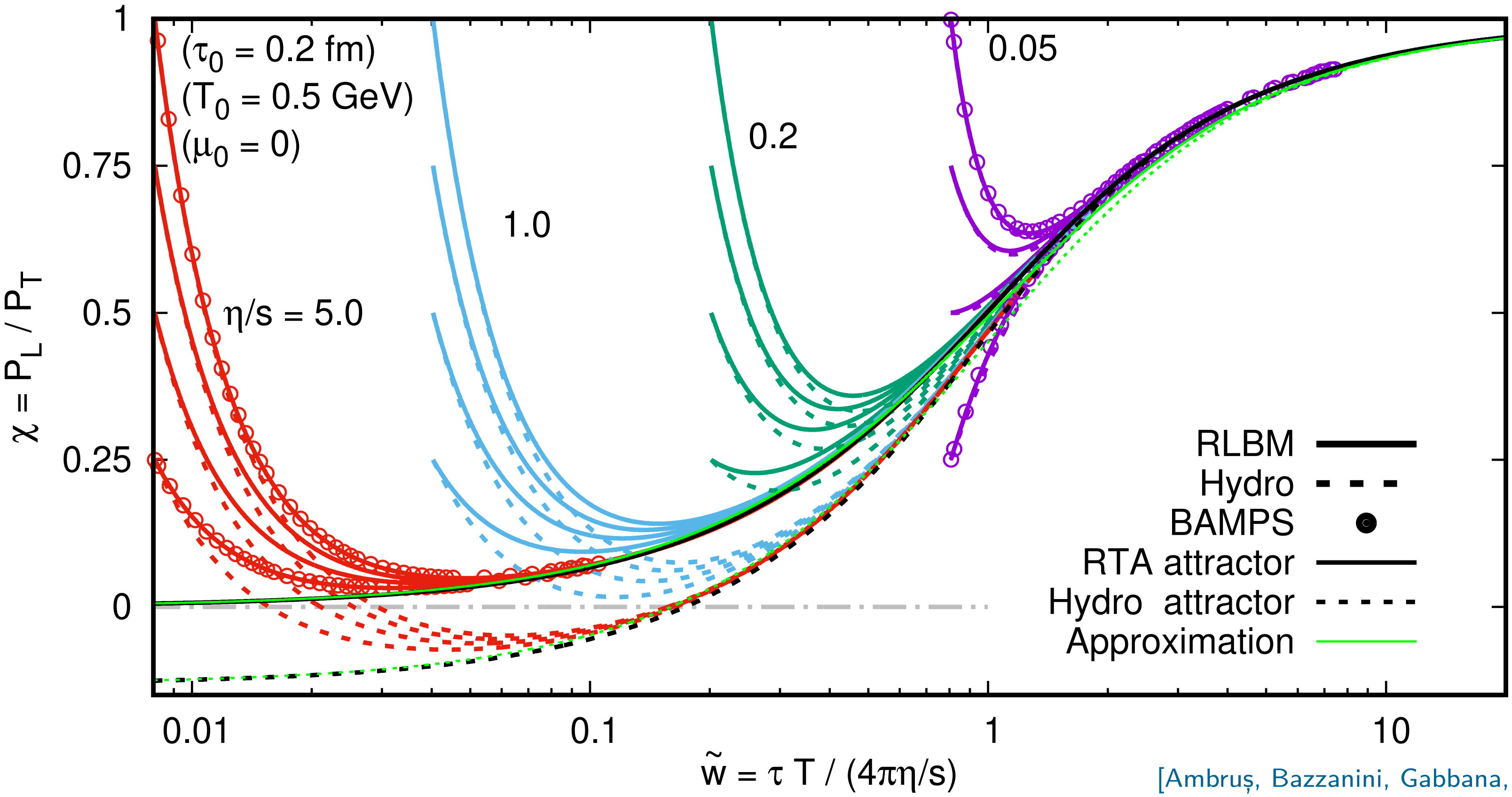

[Ambruș, Bazzanini, Gabbana, Simeoni, Succi, Nature Comput. Sci. **2** (2022) 641]

- Regularity at $\tilde{w} = 0$ selects the attractor.
- Hydro employed in HIC modelling, but it breaks down far from eq.
- Kinetic theory overcomes this limitation, but realistic simulations are expensive due to $C[f]$.

AMPT: He, Edmonds, Lin, Liu, Molnar, Wang [PLB 753 (2016) 506]
BAMPS: Greif, Greiner, Schenke, Schlichting, Xu [PRD 96 (2017) 091504]

- RTA is $1-2$ o.m. faster than BAMPS.

VEA, Busuioc, Fotakis, Gallmeister, Greiner [PRD **104** (2021) 094022]

Energy attractor

- Taking $\tau^{4/3}\epsilon(\tau) = (\tau^{4/3}\epsilon)_\infty \mathcal{E}$ and switching to $\tilde{w}$, energy conservation implies

$$\tilde{w}\left(\frac{2}{3} - \frac{f_\pi}{4}\right)\frac{d\mathcal{E}}{d\tilde{w}} + f_\pi \mathcal{E} = 0. \tag{14}$$

- $\mathcal{E} \equiv \mathcal{E}(\tilde{w})$ when f_π is a function only of $\tilde{w}$.
- The normalization is such that at late times,

$$\mathcal{E}(\tilde{w} \gg 1) = 1 - \frac{2}{3\pi\tilde{w}}, \tag{15}$$

  independent of theory.
- At early times ($\tilde{w} \ll 1$), we have

$$\mathcal{E}(\tilde{w}) = C_\infty^{-1}\tilde{w}^\gamma, \qquad \gamma = \frac{12 f_{\pi;0}}{3 f_{\pi;0} - 8} = \begin{cases} 0.526, & \text{Hydro,} \\ 4/9, & \text{RTA,} \end{cases} \tag{16}$$

  with $C_\infty \simeq 0.88$ (RTA) and 0.80 (hydro).

Attractor curves

- KT and hydro disagree far from equilibrium.
- Noneq. effects can be measured using the inverse Reynolds number,

$$\mathrm{Re}^{-1} = \sqrt{\frac{6\pi^{\mu\nu}\pi_{\mu\nu}}{\epsilon^2}}$$
$$= -3f_\pi .$$

- Hydro and KT agree when $\mathrm{Re}^{-1} \lesssim 0.75$.

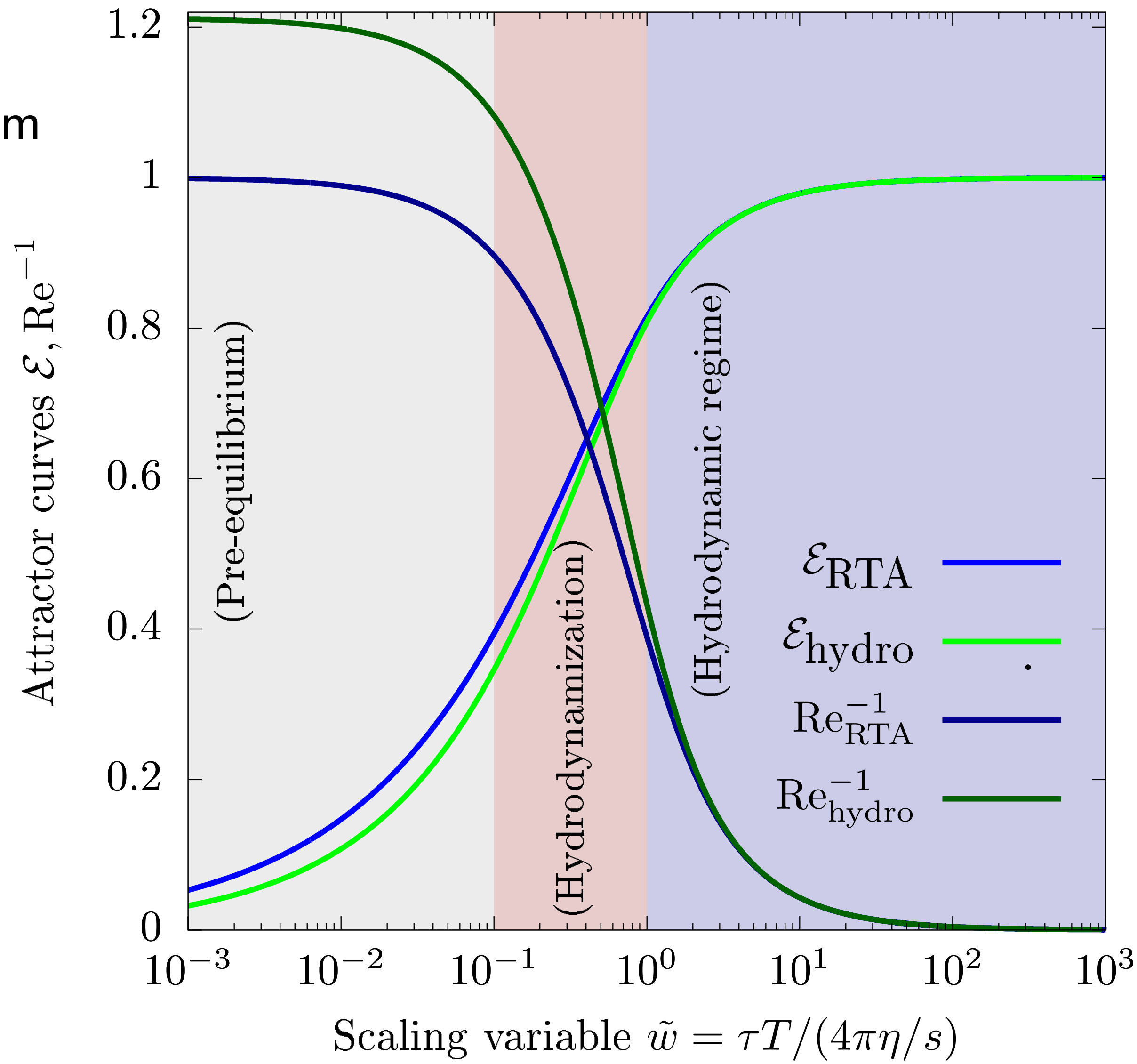

(Unphysical) early-time behavior

- Taking into account the conformal EOS, $\epsilon = aT^4$, the conformal parameter $\tilde{w}$ can be related to $\mathcal{E}(\tilde{w})$ via

$$\tilde{w} = \frac{\tau T}{4\pi\eta/s} = \frac{\tau\epsilon^{1/4}}{a^{1/4}4\pi\eta/s} = \frac{\tau^{2/3}\mathcal{E}(\tilde{w})}{a^{1/4}4\pi\eta/s}. \tag{17}$$

- At early times, $\mathcal{E}(\tilde{w}) = C_\infty^{-1}\tilde{w}^\gamma$. Solving for $\tilde{w}$ gives

$$\tilde{w} \propto \tau^{\frac{2}{3}/(1-\gamma/4)} = \begin{cases} \tau^{0.77}, & \text{Hydro,} \\ \tau^{3/4}, & \text{RKT.} \end{cases} \tag{18}$$

- Going back into $\tau^{4/3}\epsilon \propto \mathcal{E}(\tilde{w}) \propto \tilde{w}^\gamma$, we find

$$\tau^{(4/3-\gamma)/(1-\gamma/4)}\epsilon = \text{const}. \tag{19}$$

- For RKT, $\gamma = 4/9$ and $\tau\epsilon = \text{const}$.
- For Hydro, $\tau^{0.93}\epsilon = \text{const}$, such that $\tau\epsilon \propto \tau^{0.07}$.
- Unphysical early-time increase of transverse plane energy in hydro!

Early-time attractor evolution: Transverse energy

- Transverse-plane dynamics can be expected to set in when $\tau \sim R$ ($R \simeq 3$ fm).
- Much before, the evolution can be approximated as independent, point-wise Bjorken attractor evolutions.
- The transverse-plane energy at time τ can be evaluated as

$$\frac{dE_{\rm tr}}{d\eta} = \tau \int_{\mathbf{x}_\perp} (T^{xx} + T^{yy}) = \tau \int_{\mathbf{x}_\perp} \left(\frac{2}{3} - f_\pi\right) \epsilon. \tag{20}$$

- At early times, $f_\pi(\tilde{w}) \simeq f_{\pi;0} < 2/3$ and

$$\epsilon \propto \frac{\tau_0^{(4/3-\gamma)/(1-\gamma/4)}}{\tau^{(4/3-\gamma)/(1-\gamma/4)}} \epsilon_0, \tag{21}$$

  which gives

$$\left.\frac{dE_{\rm tr}}{d\eta}\right|_{\rm early} = \left(\frac{\tau_0}{\tau}\right)^{\frac{1}{3}(1-9\gamma/4)/(1-\gamma/4)} \frac{dE^0_{\rm tr}}{d\eta} = \frac{dE^0_{\rm tr}}{d\eta} \times \begin{cases} (\tau/\tau_0)^{0.07}, & \text{Hydro} \\ 1, & \text{RKT,} \end{cases} \tag{22}$$

  with $dE^0_{\rm tr}/d\eta$ being the initial transverse energy.
- Unphysical early-time increase of transverse plane energy in hydro!

Late-time agreement of transverse energy?

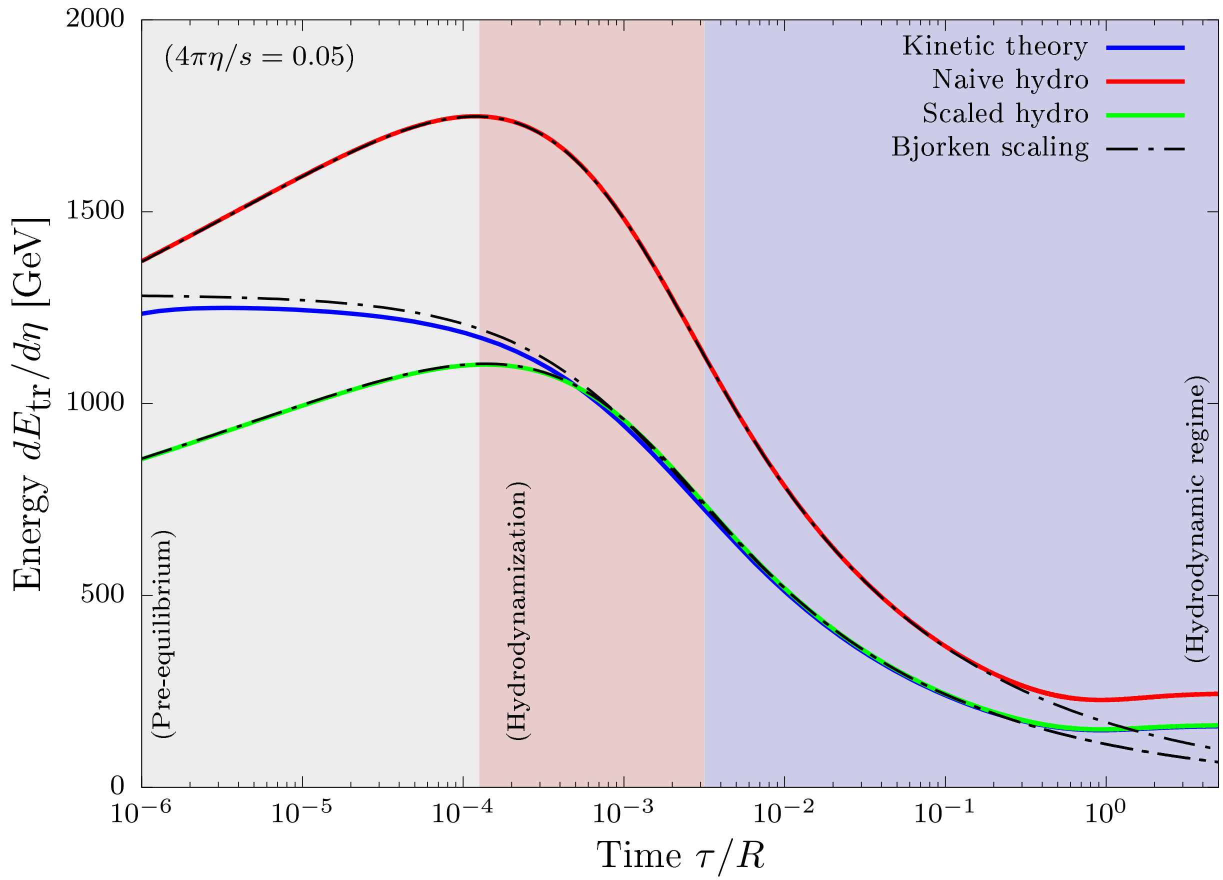

- Knowing hydro unphysically increases transverse-plane energy, let's scale down initial energy to achieve agreement.
- Is this solution enough?

Inhomogeneous cooling: Effects on geometry

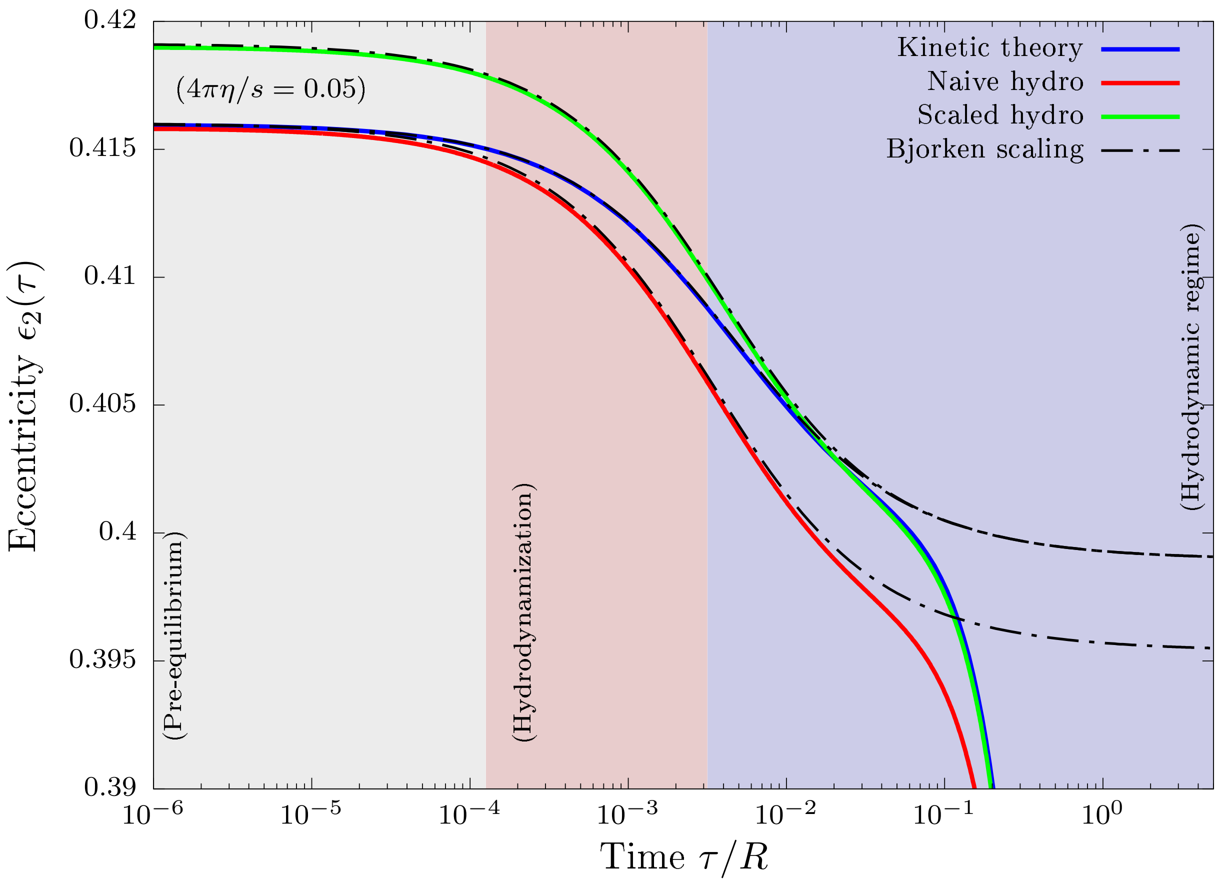

- Due to initial inhomogeneities, $\tilde{w}_0 \equiv \tilde{w}_0(\mathbf{x}_\perp)$.
- At $\tau > \tau_0$, $\tilde{w} \equiv \tilde{w}(\tau, \mathbf{x}_\perp)$ is also position-dependent.
- Each point cools at a different rate $\Rightarrow$ change in geometry!

Importance of energy attractor: from initial to final state

- The definition of the energy attractor allows us to connect the energy density ϵ_0 at initial time τ_0 to the late-time limit:

$$\tau_0^{4/3}\epsilon_0 = (\tau^{4/3}\epsilon)_\infty \mathcal{E}(\tilde{w}_0). \tag{23}$$

- when $\tilde{w}_0 \ll 1$, $\mathcal{E}(\tilde{w}_0) = C_\infty^{-1}\tilde{w}_0^\gamma$.
- By definition,

$$\tilde{w}_0 = \frac{\tau_0 T_0}{4\pi\eta/s}, \tag{24}$$

- The conformal EOS $\epsilon_0 = aT_0^4$ allows $\tilde{w}_0$ to be expressed as

$$\tilde{w}_0 = \frac{\tau_0 \epsilon_0^{1/4}}{a^{1/4} 4\pi\eta/s}. \tag{25}$$

- This leads to a relation between final- and initial-state energies:

$$(\tau^{4/3}\epsilon)_\infty = \left(\frac{4\pi\eta}{s}a^{1/4}\right)^\gamma \left(\tau_0^{(\frac{4}{3}-\gamma)/(1-\frac{\gamma}{4})}\epsilon_0\right)^{1-\gamma/4}. \tag{26}$$

(Local) Attractor scaling of hydro

- Due to the pre-equilibrium evolution, $\varepsilon_2(\tau = \tau_T) \neq \varepsilon_2(\tau = \tau_0)$.
- Discarding early-time hydro evolution as unphysical, we demand

$$\lim_{\tau\to\infty} \epsilon_{\text{hydro}}(\tau) = \lim_{\tau\to\infty} \epsilon_{\text{RKT}}(\tau). \tag{27}$$

- Knowing the relation between $(\tau^{4/3}\epsilon)_\infty$ and ϵ_0, hydro agrees with RKT at late times if:

$$\epsilon_{0,\text{hydro}} = \left[\left(\frac{4\pi\eta/s}{\tau_0} a^{1/4} \right)^{\frac{1}{2}-\frac{9\gamma}{8}} \left(\frac{C_{\infty,\text{RTA}}}{C_{\infty,\gamma}} \right)^{9/8} \epsilon_{0,\text{RTA}} \right]^{\frac{8/9}{1-\gamma/4}}. \tag{28}$$

- The ideal hydro limit can be taken by noting that $\tau^{4/3}\epsilon_{\text{id.}}(\tau) = \tau_0^{4/3}\epsilon_0$ $(\gamma = 0)$:

$$\epsilon_{0,\text{id.}} = a^{1/9} \left(\frac{4\pi\eta}{s} \right)^{4/9} C_{\infty,\text{RTA}} \tau_0^{-4/9} \epsilon_{0,\text{RTA}}^{8/9}, \tag{29}$$

where η/s acts as a free parameter to tune e.g. the final $dE_\perp/d\eta$, reminiscent of the absence of free-streaming in the $\tau \to 0$ limit of ideal hydro.

Fixing the preequilibrium discrepancies

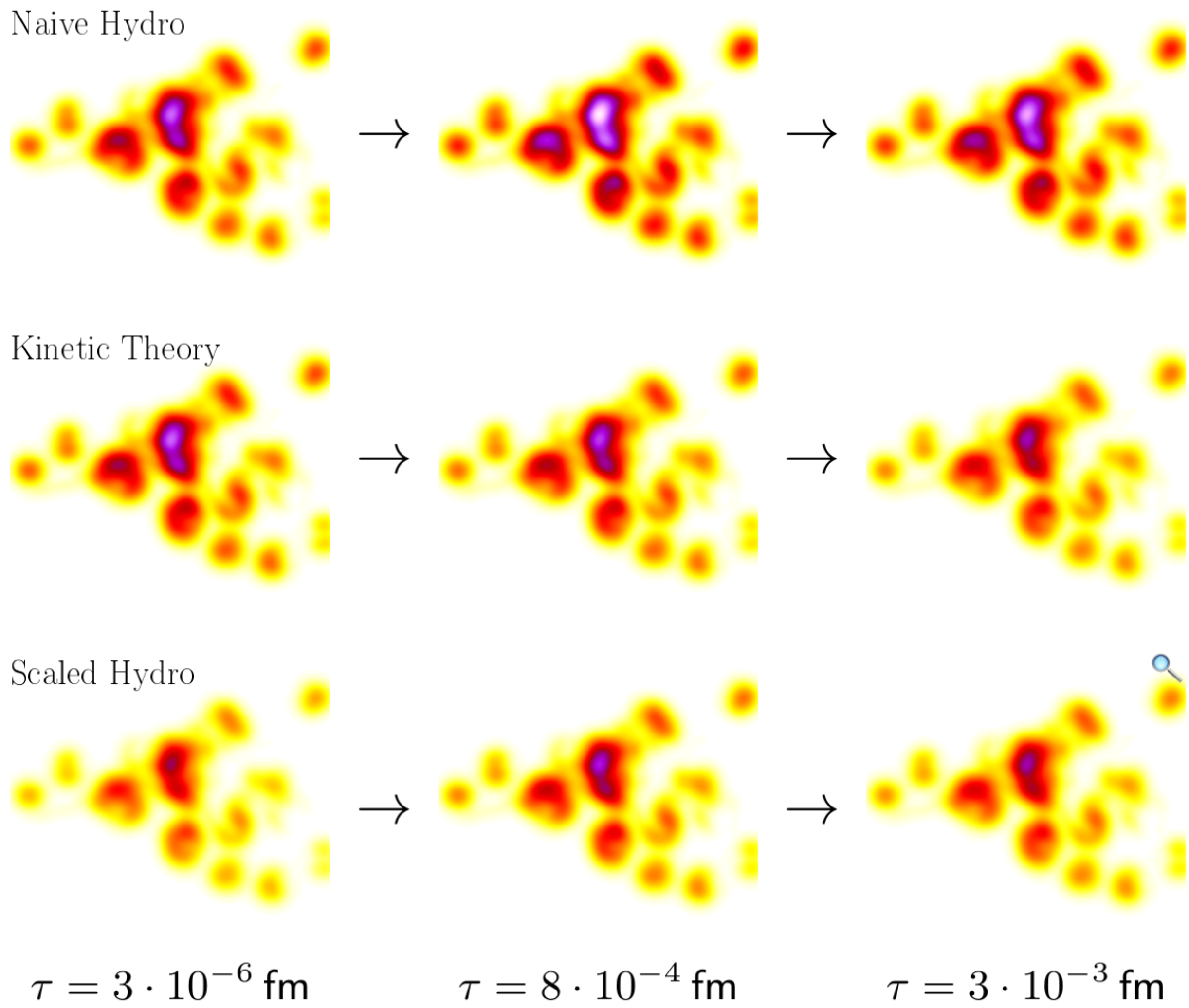

- Preeq. discrepancies counteracted using modified, locally-scaled $\epsilon_0^{\text{hydro}}(\mathbf{x}_\perp)$.
  - Fails when eq. time $\tau_{\text{eq}} \sim \hat{\gamma}^{-4/3}$ is comparable to R and eq. is interrupted by transverse expantion!
- Hybrid simulations, switching from KT to hydro at $\tau_{\text{sw}} > \tau_0$?

Transition between dynamical regimes

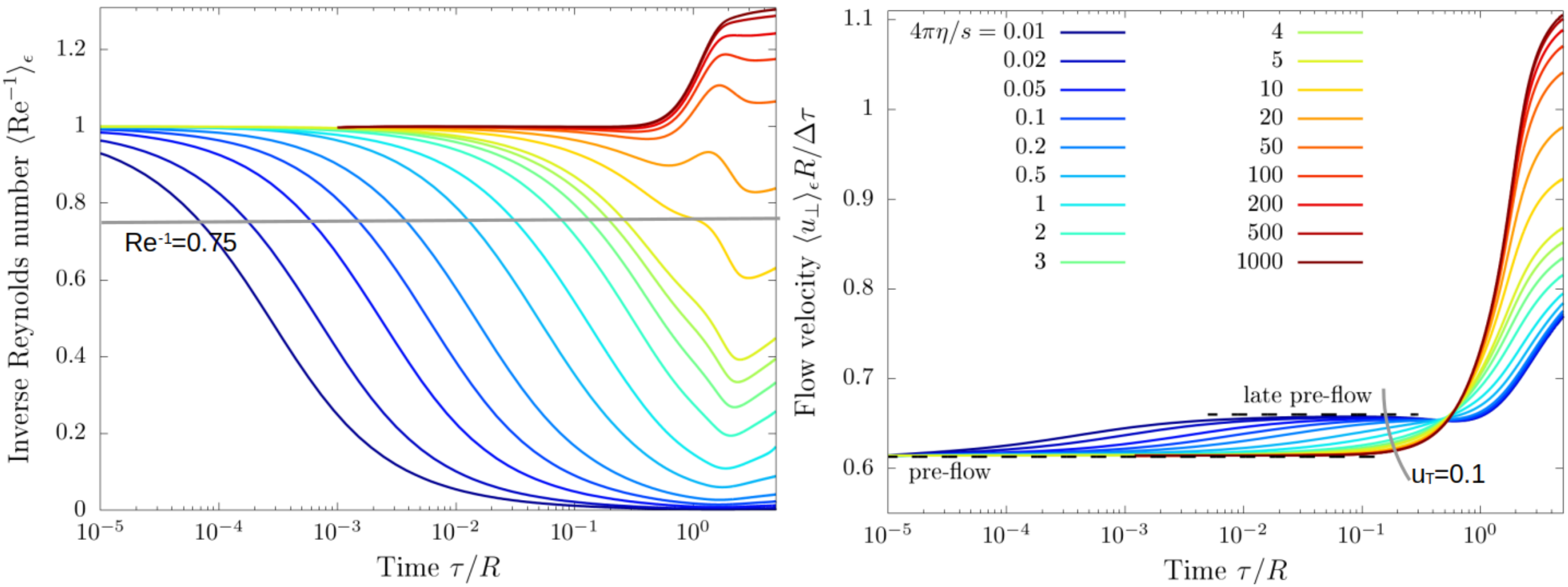

- Transverse expansion sets in when $\langle u_\perp \rangle_\epsilon \gtrsim 0.1$, for $\tau \simeq 0.2R$.
- Hydro is applicable when $\mathrm{Re}^{-1} \lesssim 0.75 \Rightarrow$ discrepancies can be expected for $4\pi\eta/s \gtrsim 3$.

Fixing the preequilibrium discrepancies

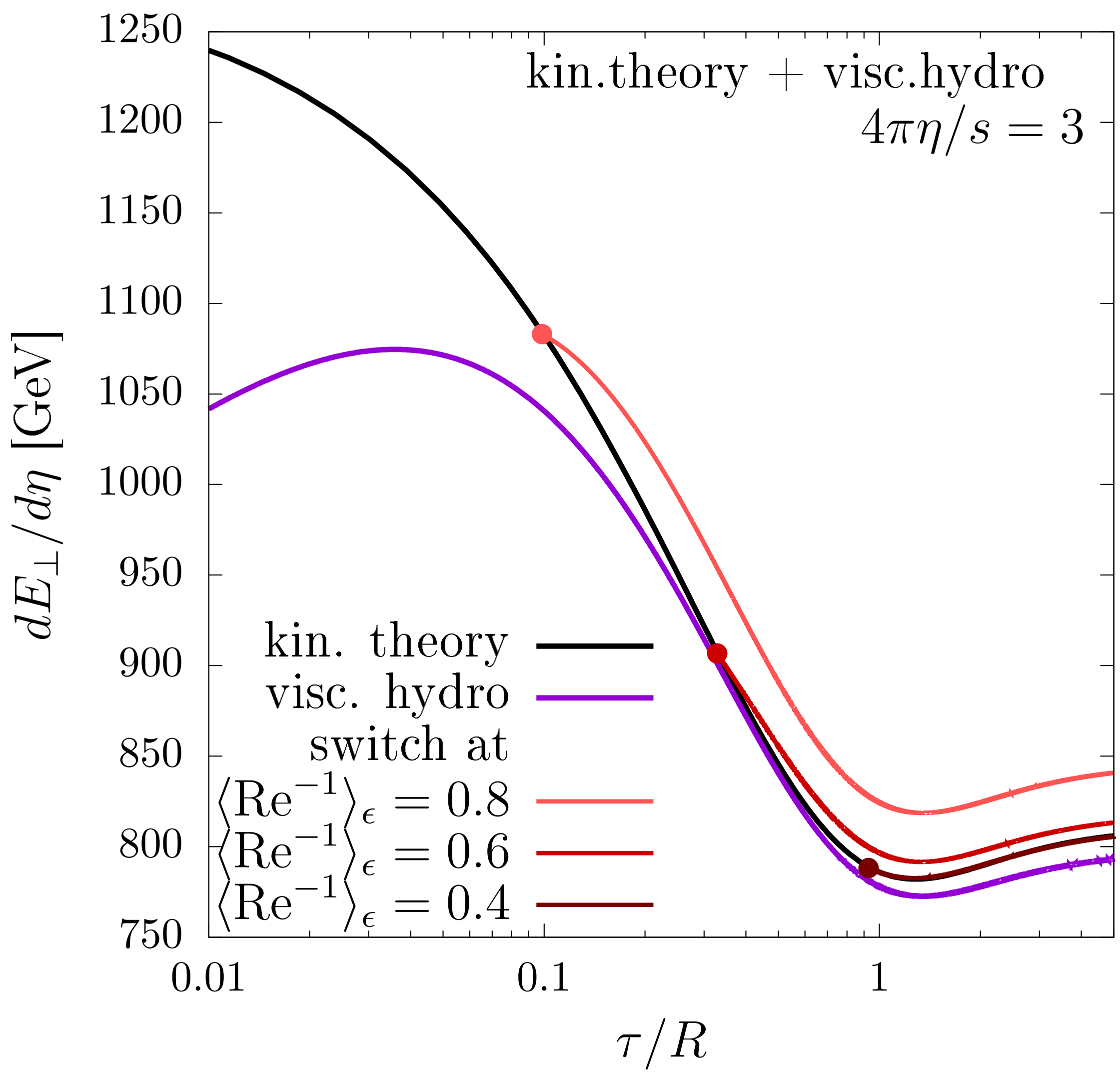

- Hybrid simulations, switching from KT to hydro at $\tau_{\rm sw} > \tau_0$.
  - When $\mathrm{Re}^{-1}(\tau_{\rm sw}) \gtrsim 0.4$, part of the system is still in preeq. ⇒ discrepancies will appear at late times ⇒ $\mathrm{Re}^{-1}(\tau_{\rm sw})$-based criterion!
  - For small $\hat{\gamma}$, $\mathrm{Re}^{-1}(\tau_{\rm eq})$ is still large ⇒ Re^{-1}-based switching criterion is never reached!

Scaled and hybrid hydro vs. KT

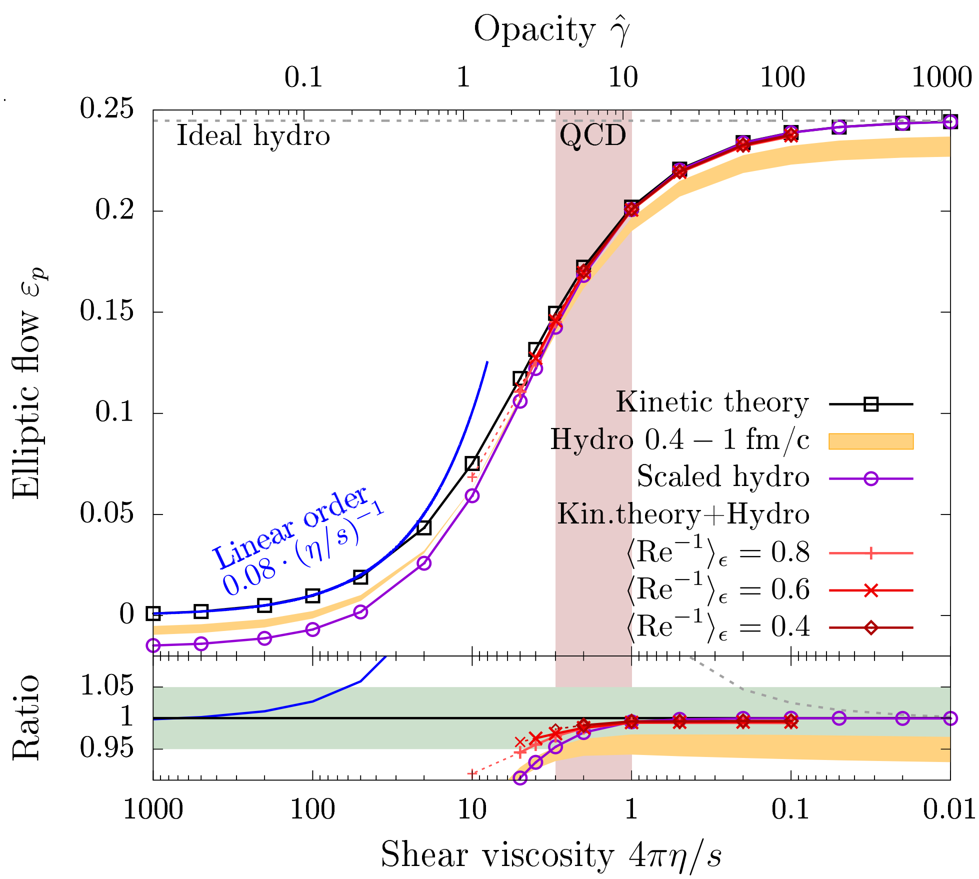

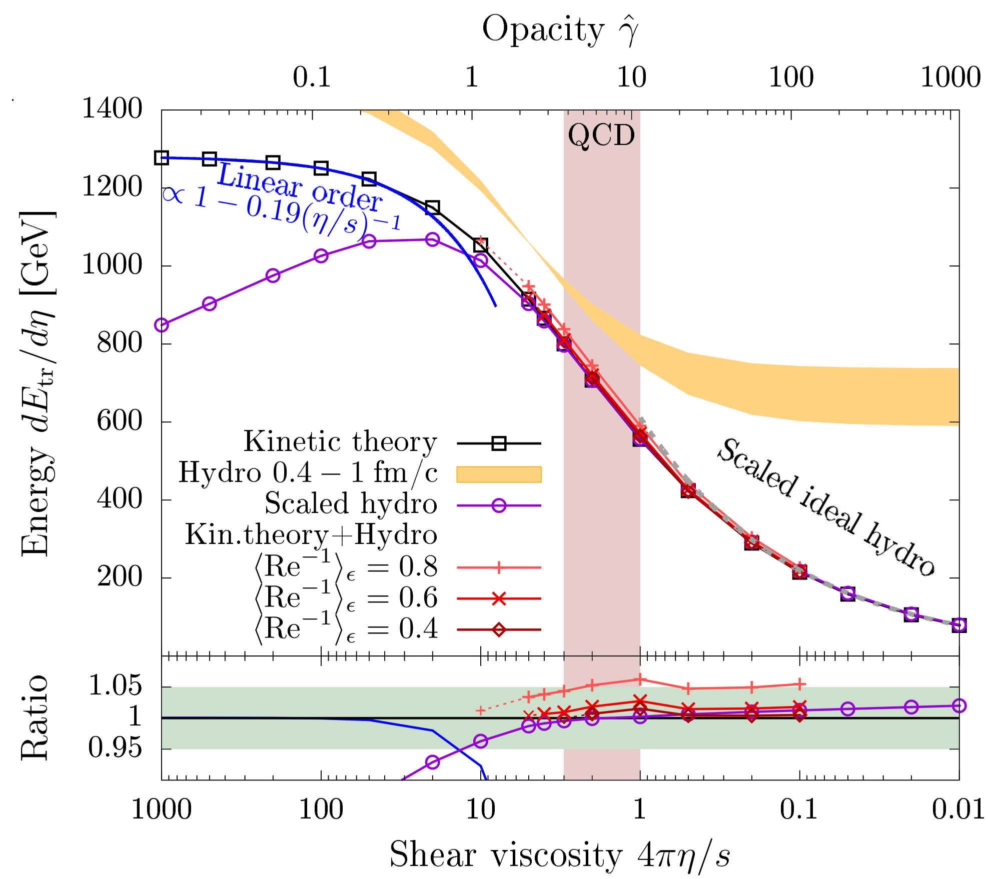

- Naive hydro, initialized with same ϵ_0 as RKT at $\tau_0 = 0.4$–$1\ \mathrm{fm}/c$ underestimates ε_p and overestimates $dE_{\mathrm{tr}}/d\eta$.
- Scaled hydro is in perfect agreement at large $\hat{\gamma}$ but loses applicability as $\hat{\gamma} \lesssim 3$–4.
- Hybrid hydro can improve on scaled hydro, but only down to $\hat{\gamma} \simeq 1$.

Regime of applicability of hydrodynamics

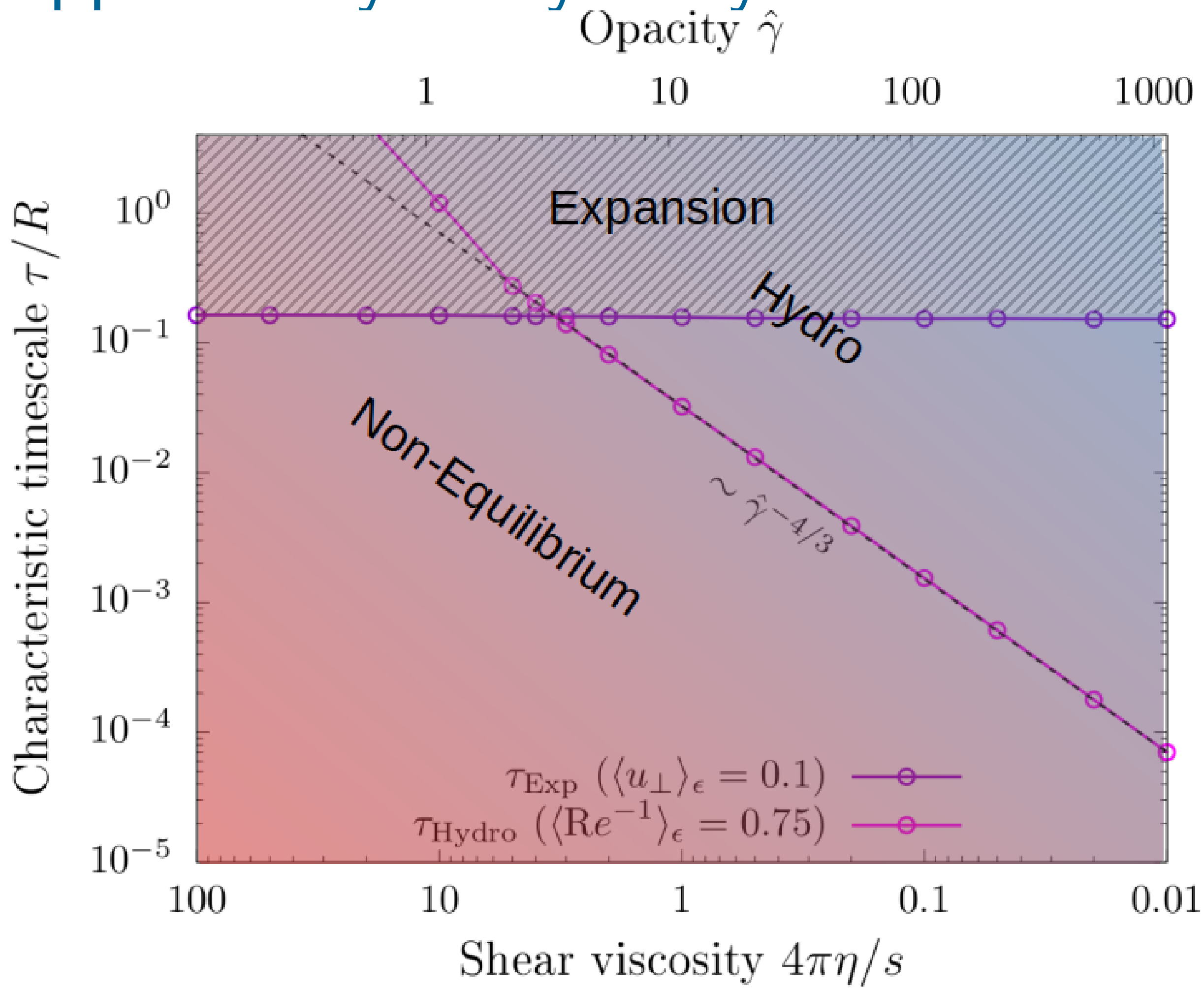

- Transverse expansion sets in at $\tau_{\mathrm{Exp}} \sim 0.2R$, independent of opacity.
- Hydro applicable when $\mathrm{Re}^{-1} \lesssim 0.75$.
- When $\hat{\gamma} \lesssim 3$, hydrodynamization is interrupted by transv. expansion.

Hydrodynamics in real collision systems

What does the criterion $\hat{\gamma} \gtrsim 3$ imply for the applicability of hydro to realistic collisions?

$$\mathrm{p+p}: \hat{\gamma} \sim \overset{\text{min.bias}}{0.7} \left(\frac{\eta/s}{0.16}\right)^{-1} \left(\frac{R}{0.12\,\mathrm{fm}}\right)^{1/4} \left(\frac{\mathrm{d}E_\perp^{(0)}/\mathrm{d}\eta}{7.1\,\mathrm{GeV}}\right)^{1/4} \left(\frac{\nu_{\mathrm{eff}}}{42.25}\right)^{-1/4}$$

far from hydrodynamic behaviour

$$\mathrm{p+Pb}: \hat{\gamma} \sim \overset{\text{min.bias}}{1.5} \left(\frac{\eta/s}{0.16}\right)^{-1} \left(\frac{R}{0.81\,\mathrm{fm}}\right)^{1/4} \left(\frac{\mathrm{d}E_\perp^{(0)}/\mathrm{d}\eta}{24\,\mathrm{GeV}}\right)^{1/4} \left(\frac{\nu_{\mathrm{eff}}}{42.25}\right)^{-1/4} \overset{\text{high mult.}}{\lesssim 2.7}$$

very high multiplicity events approach regime of applicability, but do not reach it

$$\mathrm{O+O}: \hat{\gamma} \sim \overset{30-40\%}{2.2} \left(\frac{\eta/s}{0.16}\right)^{-1} \left(\frac{R}{1.13\,\mathrm{fm}}\right)^{1/4} \left(\frac{\mathrm{d}E_\perp^{(0)}/\mathrm{d}\eta}{55\,\mathrm{GeV}}\right)^{1/4} \left(\frac{\nu_{\mathrm{eff}}}{42.25}\right)^{-1/4} \sim \overset{70-80\%}{1.4} - \overset{0-5\%}{3.1}$$

probes transition region to hydrodynamic behaviour

$$\mathrm{Pb+Pb}: \hat{\gamma} \sim \overset{30-40\%}{5.7} \left(\frac{\eta/s}{0.16}\right)^{-1} \left(\frac{R}{2.78\,\mathrm{fm}}\right)^{1/4} \left(\frac{\mathrm{d}E_\perp^{(0)}/\mathrm{d}\eta}{1280\,\mathrm{GeV}}\right)^{1/4} \left(\frac{\nu_{\mathrm{eff}}}{42.25}\right)^{-1/4} \sim \overset{70-80\%}{2.7} - \overset{0-5\%}{9.0}$$

hydrodynamic behaviour in all but peripheral collisions

Limitations of current approach

- The "scaled hydro" argument rests on an analytical knowledge of the attractor – known in a limited number of cases!
- Effects due to non-ideal EOS ignored!
- Effects due to finite mass (non-conformal) ignored!
- Realistic (bulk) viscosities ignored!
- Bjorken attractor loses validity if the system is not boost-invariant.
- Can RTA go beyond current model?
  - Non-ideal ✓ [P. Romatschke, PRD **85** (2012) 065012]
  - Non-conformal ✓ [PRD **109** (2024) 076001, PRD **110** (2024) 056002]
  - Realistic transport coefficients ✓ [PLB **855** (2024) 138795, PRD **110** (2024) 056002]
  - Full $3+1$D ✓ [Nature Comput. Sci. **2** (2022) 641]

Summary

- We employed KT to explore transverse flow for a simplified, conformal fluid over the entire opacity range.
- Hydrodynamics is accurate at 5% level if Re^{-1} drops below ~ 0.75 before transverse expansion sets in.
- In small systems (p+p, p+Pb), transverse expansion interrupts equilibration ⇒ hydro not applicable!
  - O+O covers transition regime to hydro behaviour

- Support through the DEVELOP grant awarded by the West University of Timișoara is gratefully acknowledged.

Appendix

Attractor solution ($\mu = 0$)

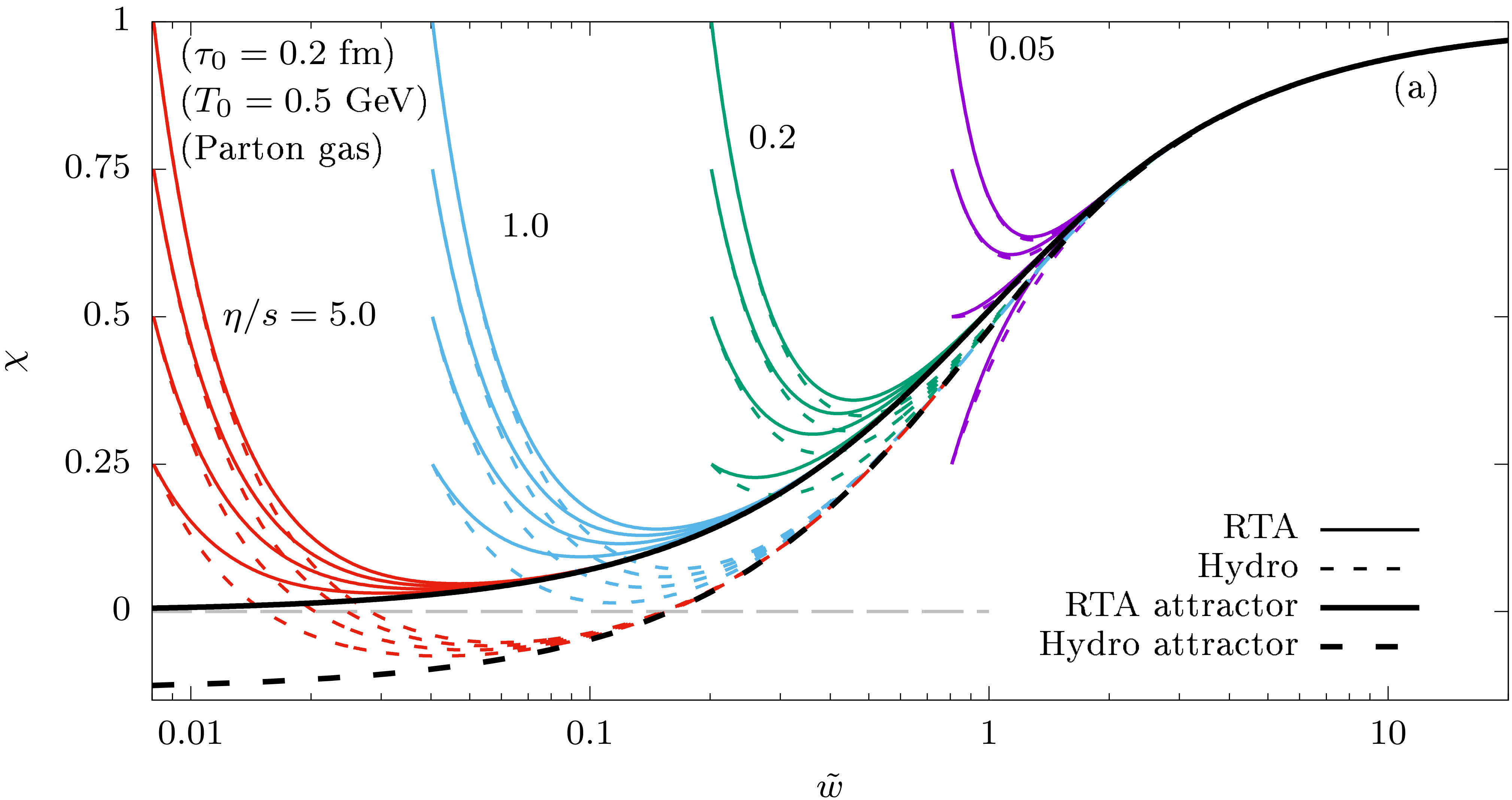

- Regularity at $\tilde{w} = 0$ selects the attractor.
- Solutions initialised at various $\tilde{w}_0$ decay towards the attractor.
- Hydro casually gives negative $\chi = \mathcal{P}_L/\mathcal{P}_T$.

Attractor for $\mu \neq 0$

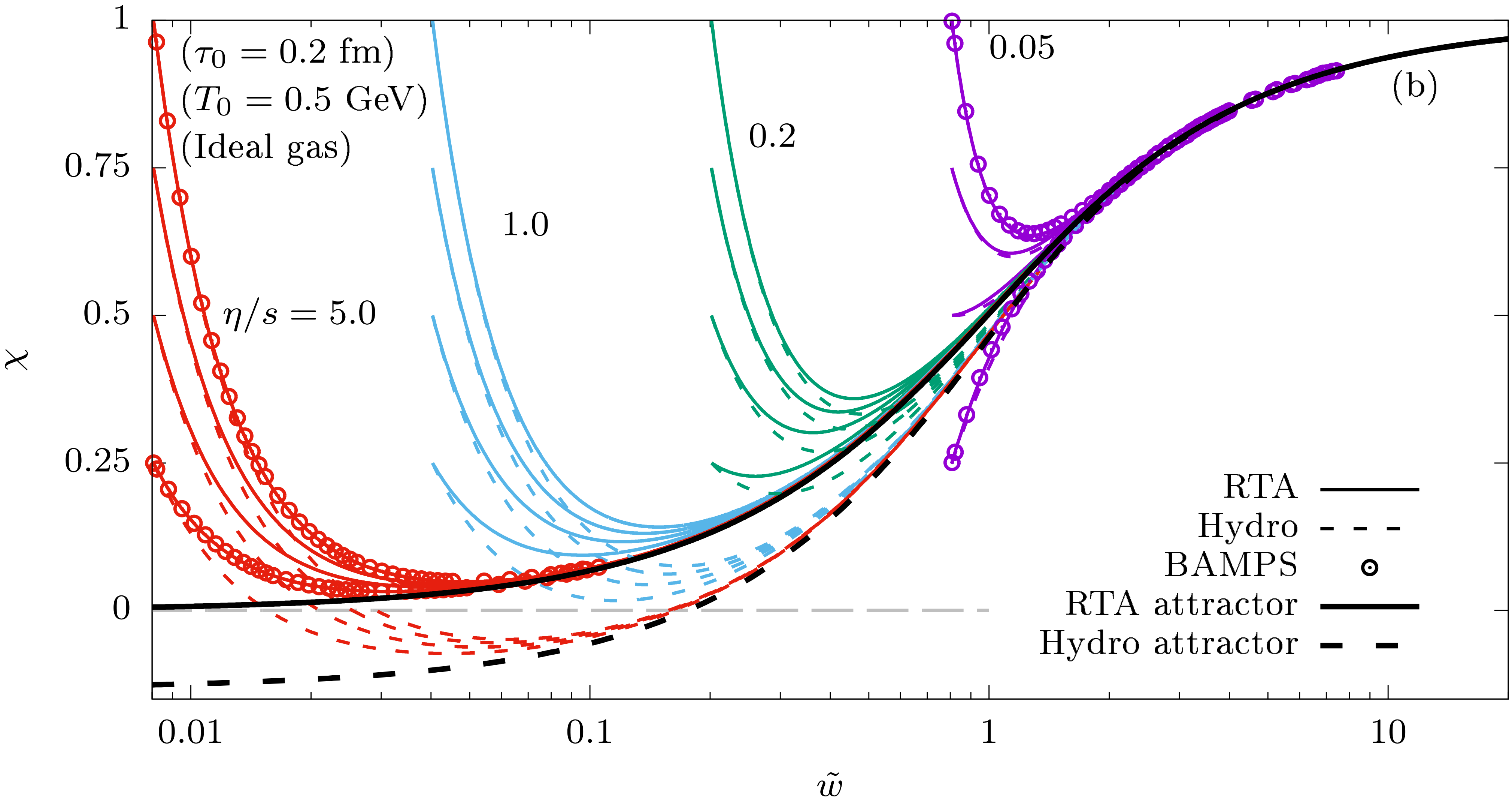

$$\tilde{w} = \frac{5\tau}{4\pi\tau_R} = \frac{\tau T}{4\pi\eta/s}\left[1 - \frac{\alpha_0}{4} + \frac{3}{4}\ln\frac{\tau^{4/3}P}{\tau_0^{4/3}P_0}\right]. \quad (30)$$

- RTA validated against BAMPS.

Attractor for HS

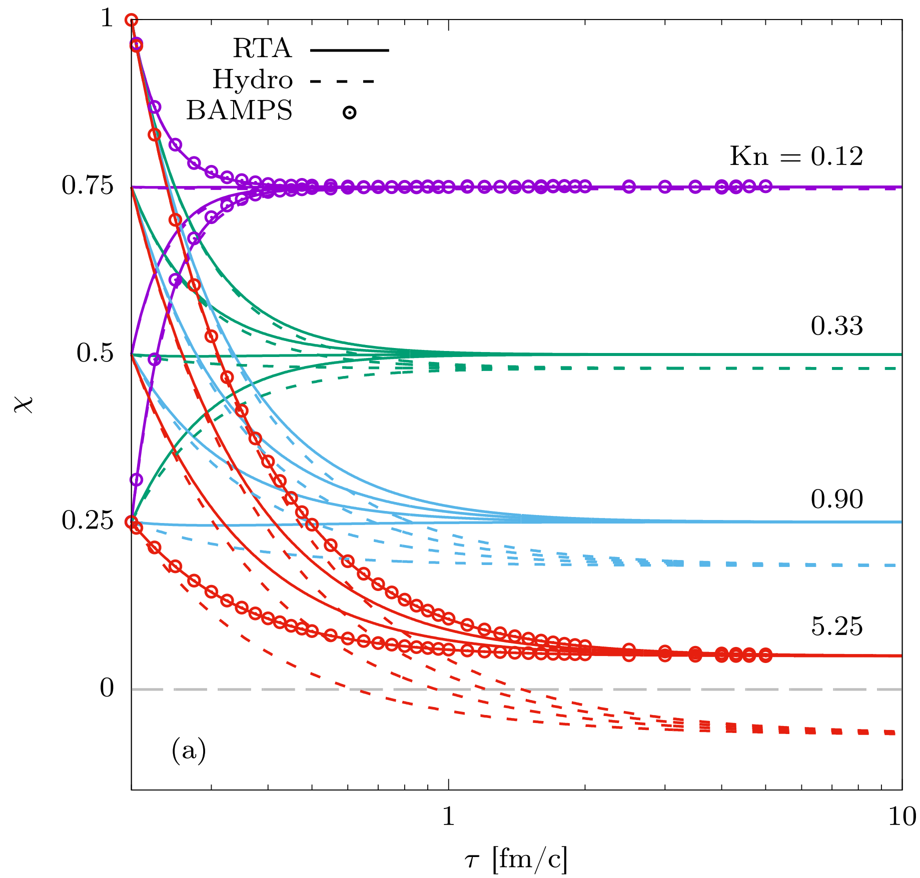

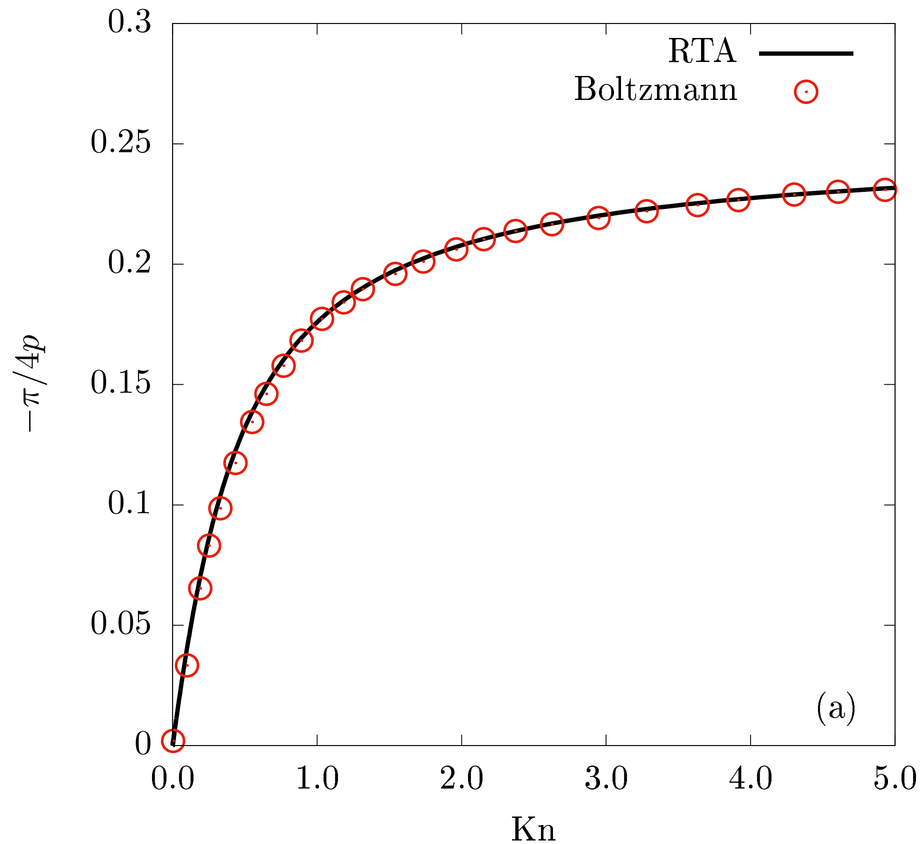

- Attractor-like behaviour confirmed also for hard spheres, $\eta = 1.2654 T/\sigma$.
- Here, $\tau_R = 5\eta/4P \sim \tau$, such that

$$\tilde{w} = \frac{1}{1.2654\pi \text{ Kn}} = \text{const}, \qquad \text{Kn} = \frac{1}{\tau n \sigma} = \frac{1}{\tau_0 n_0 \sigma}. \tag{31}$$

Attractor for HS

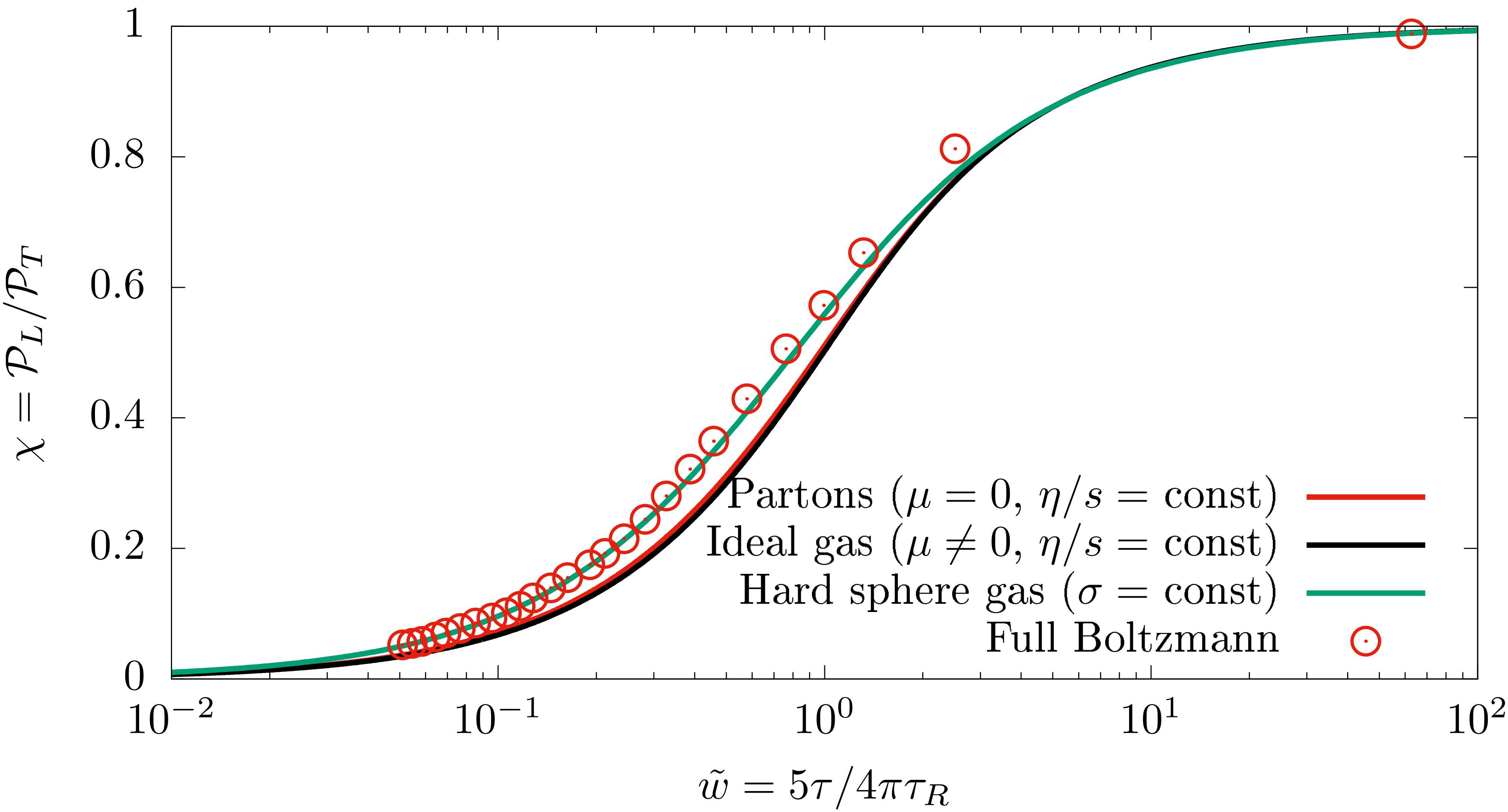

- For HS, the system stays at the same $\tilde{w} \Rightarrow \chi(\tilde{w})$ can be obtained by considering multiple systems.
- $\chi(\tilde{w})$ is very similar for partons vs ideal vs HS.

Setup

- microscopic description in terms of averaged on-shell phase-space distribution:

$$f(\tau, \mathbf{x}_\perp, \eta, \mathbf{p}_\perp, y) = \frac{(2\pi)^3}{\nu_{\text{eff}}} \frac{\mathrm{d}N}{\mathrm{d}^3x\,\mathrm{d}^3p}(\tau, \mathbf{x}_\perp, \eta, \mathbf{p}_\perp, y) \tag{32}$$

  - boost invariance: $(2+1)+3$D description
- time evolution: Boltzmann equation in relaxation time approximation

$$p^\mu \partial_\mu f = C_{RTA}[f] = \frac{p_\mu u^\mu}{\tau_R}(f_{eq} - f)\ , \quad \tau_R = 5\frac{\eta}{s}T^{-1} \tag{33}$$

- specify initial energy density to be isotropic Gaussian with anisotropic perturbation

$$\epsilon(\tau_0, \mathbf{x}_\perp) = \frac{\mathrm{d}E_\perp^{(0)}}{\mathrm{d}\eta} \frac{1}{\pi R^2 \tau_0} \exp\left(-\frac{x_\perp^2}{R^2}\right)\left\{1 + \delta_n \exp\left(-\frac{x_\perp^2}{2R^2}\right)\left(\frac{x_\perp}{R}\right)^n \cos(n\phi_x)\right\} \tag{34}$$

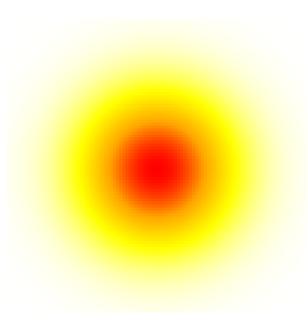

(no ecc.)

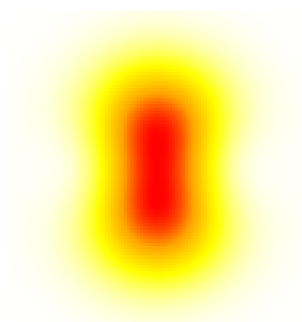

$(n=2)$

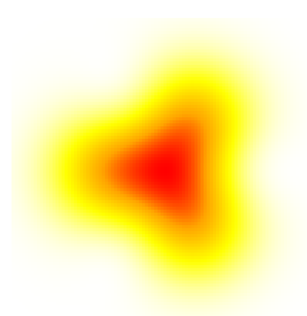

$(n=3)$

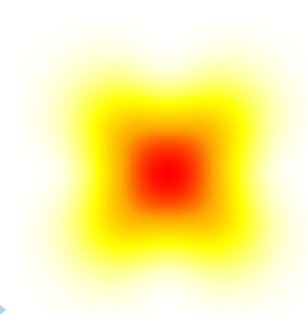

$(n=4)$

Eccentricity Dependence

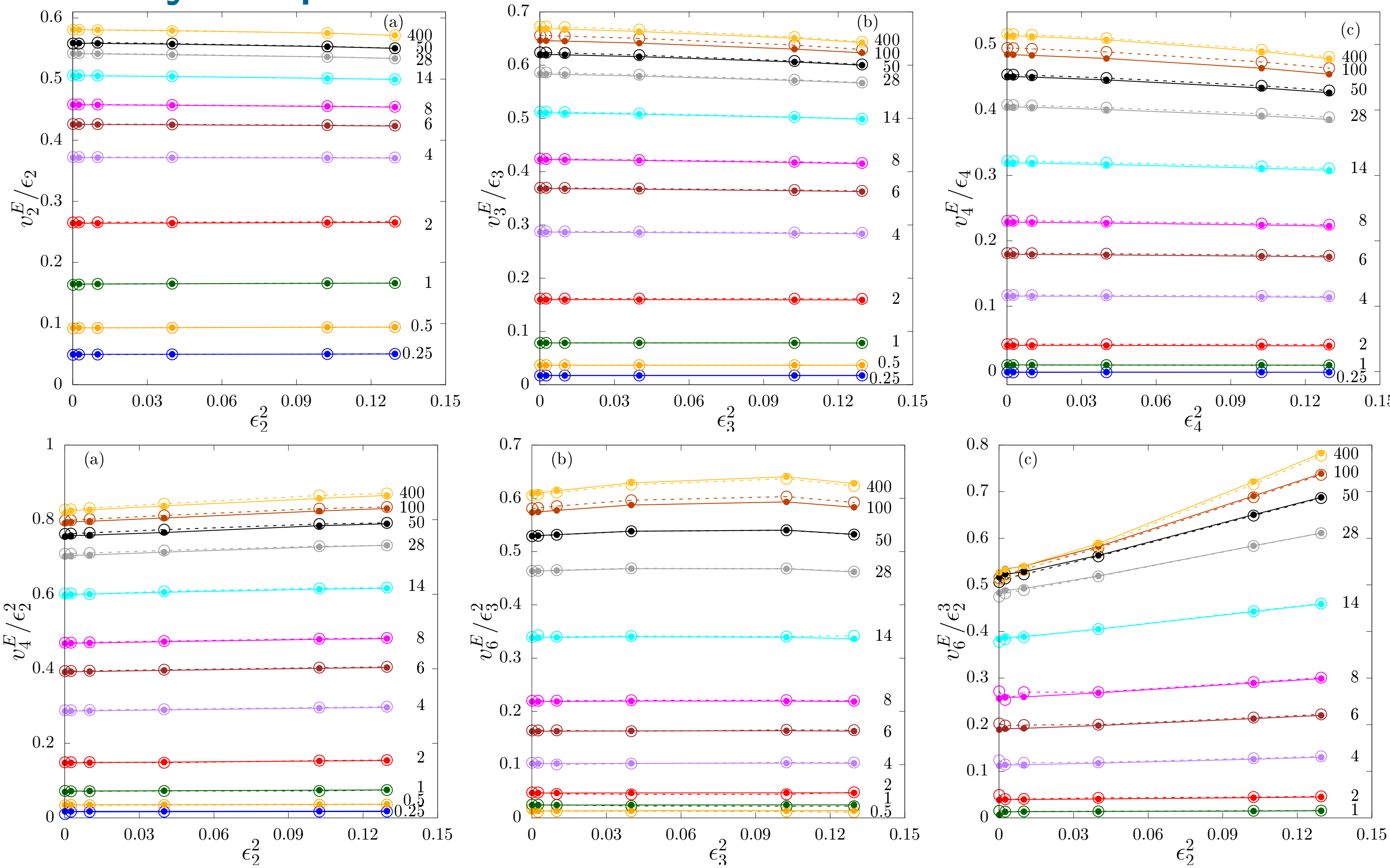

- almost no ϵ_n-dependence, only small negative/positive trend (except cubic response)
- in conflict with conventional knowledge (upwards trend); even in identical setup

Niemi, Eskola, Paatelainen PRC 93 (2016) 024907 Kurkela, Taghavi, Wiedemann, Wu PLB 811 (2020) 135901

- cross-checked this also with e.g. hydro
  - attributed to other features of specific initial state; not fully described by ϵ_n?

Opacity Dependence

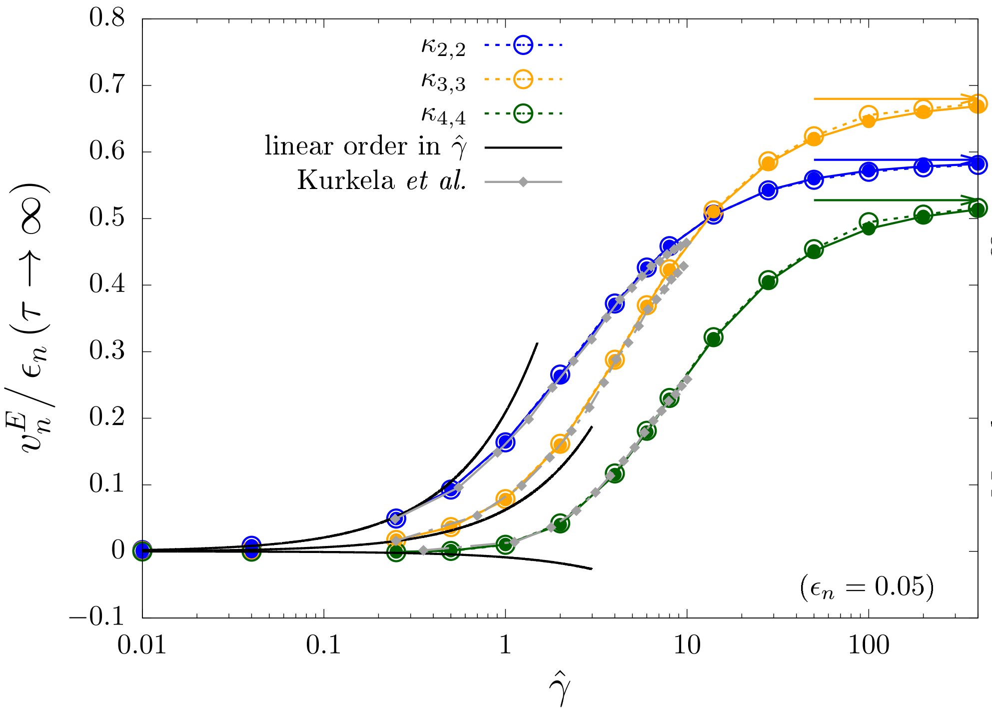

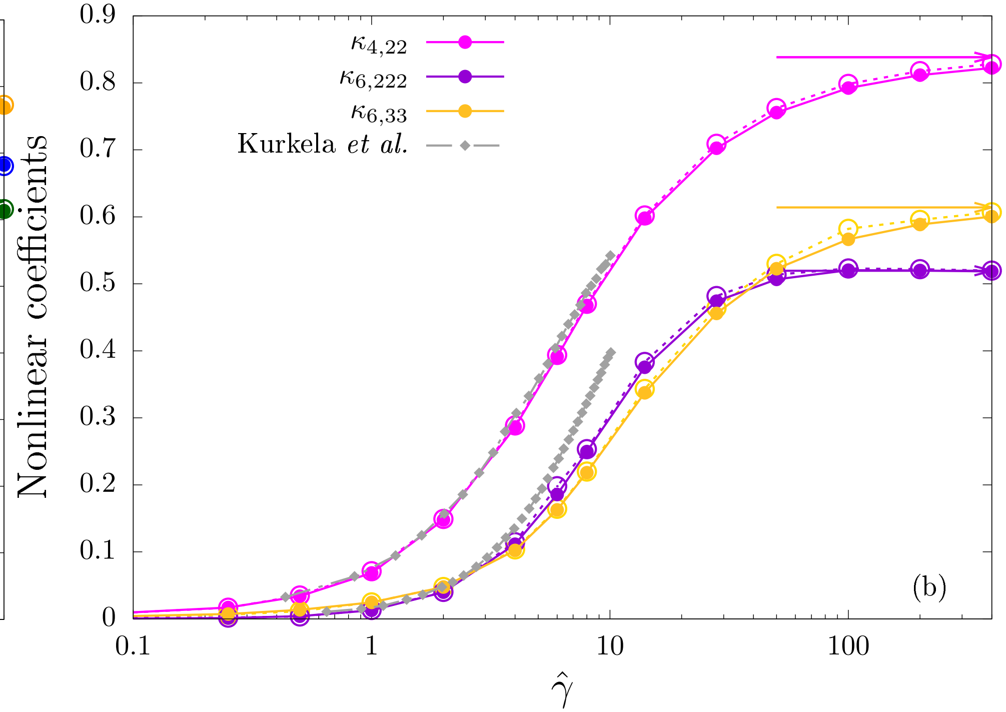

- linear order results have different ranges of validity for different v_n due to peculiarities of small-$\hat{\gamma}$-behaviour
- agreement with previous results in identical setup up to moderate $\hat{\gamma}$

Kurkela, Taghavi, Wiedemann, Wu PLB 811 (2020) 135901

- extension to higher $\hat{\gamma}$, clear signs of saturation

Pre-equilibrium "running" of eccentricity

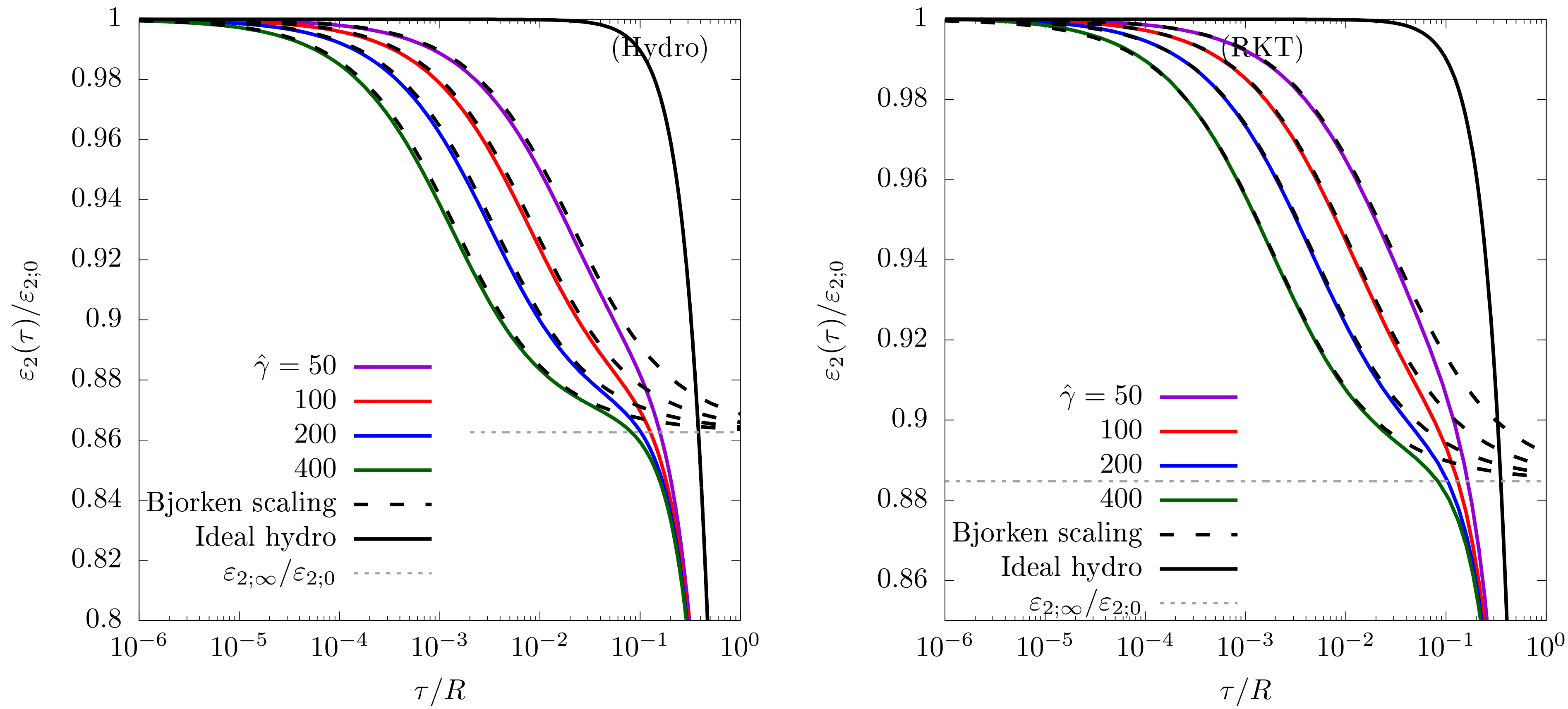

- Due to inhomogeneous cooling, eccentricity decays in pre-equilibrium phase.
- The full $0+1$D "running" of ε_n is: $[\gamma_{\rm RKT} = 4/9,\ \gamma_{\rm MIS} \simeq 0.526]$

$$\frac{\varepsilon_n(\tau \to \infty)}{\varepsilon_n(\tau \to 0)} = \frac{\left(1 - \frac{\gamma}{4}\right)^{\frac{n}{2}+2}}{\left(1 - \frac{\gamma}{6}\right)^{n+1}}. \tag{35}$$

Attractro scaling of hydro

- Due to the pre-equilibrium evolution, $\varepsilon_2(\tau = \tau_T) < \varepsilon_2(\tau = \tau_0)$.
- Since ε_n running is different for hydro than for RKT, the response in ϵ_p will also be different.
- The solution is to acknowledge that the pre-equilibrium evolution is governed by the attractor solution,

$$\tau^{\frac{\frac{4}{3}-\gamma}{1-\gamma/4}} e \sim \text{const.}$$

- A way to cure the hydro vs RKT discrepancy is to perform "backwards running" on hydro, such that hydro and RKT agree in the "hydro" regime (when $\tilde{w} \to \infty$):

$$\lim_{\tau\to\infty} e_{\text{hydro}}(\tau) = \lim_{\tau\to\infty} e_{\text{RKT}}(\tau). \quad (36)$$

Attractro scaling of hydro

- In general, one may write

$$e(\tau) = e_\infty \mathcal{E}(\tilde{w}), \qquad e_\infty = aT_\infty^4, \qquad T_\infty = 4\pi(\eta/s)\tilde{w}_\infty/\tau, \tag{37}$$

where $\tilde{w}_\infty$ depends on γ ($= 4/9$ for RKT and $\simeq 0.526$ for hydro):

$$\tilde{w}_\infty = \frac{\mathcal{E}^{1/4}(\tilde{w})}{\tilde{w}} = \left(\tau_0^{(\frac{1}{3}-\frac{\gamma}{4})/(1-\gamma/4)} \frac{(e_0/a)^{1/4}}{4\pi\eta/s}\right)^{1-\gamma/4} C_\infty^{1/4}\tau^{2/3}. \tag{38}$$

- Since $\mathcal{E}(\tilde{w}) \to 1$ when $\tilde{w} \to 1$, matching is ensured if $\tilde{w}_\infty^{\mathrm{hydro}} = \tilde{w}_\infty^{\mathrm{RKT}}$, leading to

$$e_{0,\gamma} = \left[\left(\frac{4\pi\eta/s}{\tau_0} a^{1/4}\right)^{\frac{1}{2}-\frac{9\gamma}{8}} \left(\frac{C_{\infty,\mathrm{RTA}}}{C_{\infty,\gamma}}\right)^{9/8} e_{0,\mathrm{RTA}}\right]^{\frac{8/9}{1-\gamma/4}}. \tag{39}$$

- The ideal hydro limit can be taken by noting that $e_{\mathsf{ideal}}(\tau) = e_0\tau_0^{4/3}/\tau^{4/3}$:

$$e_{0,\mathsf{ideal}} = a^{1/9}\left(\frac{4\pi\eta}{s}\right)^{4/9} C_{\infty,\mathrm{RTA}}\tau_0^{-4/9} e_{0,\mathrm{RTA}}^{8/9}, \tag{40}$$

where η/s acts as a free parameter to tune e.g. the final $dE_\perp/d\eta$, reminiscent of the absence of free-streaming in the $\tau \to 0$ limit of ideal hydro.

Attractro scaling of hydro

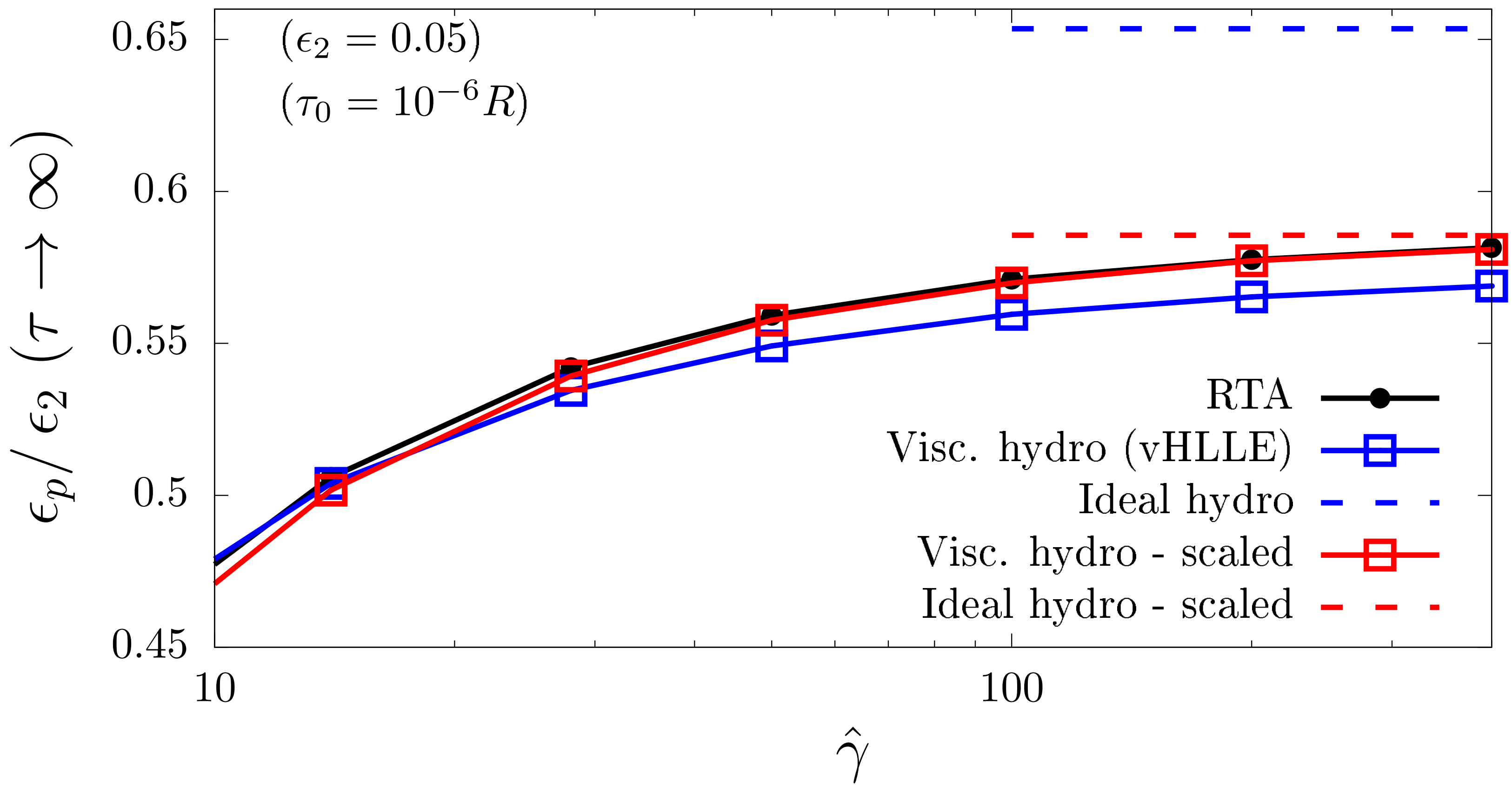

- vHLLE and RTA are in excellent agreement at large $\hat{\gamma}$.
- The ideal hydro limit now agrees with the $\hat{\gamma} \to \infty$ of both RTA and vHLLE.

Naïve hydro: Opacity Dependence in Comparison to Hydro

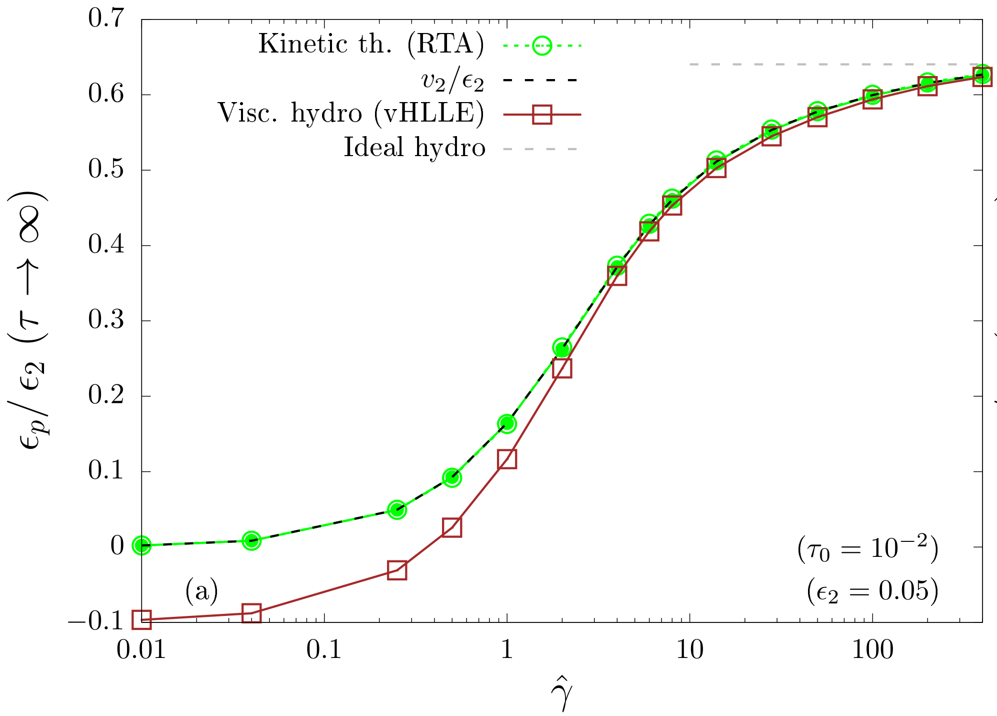

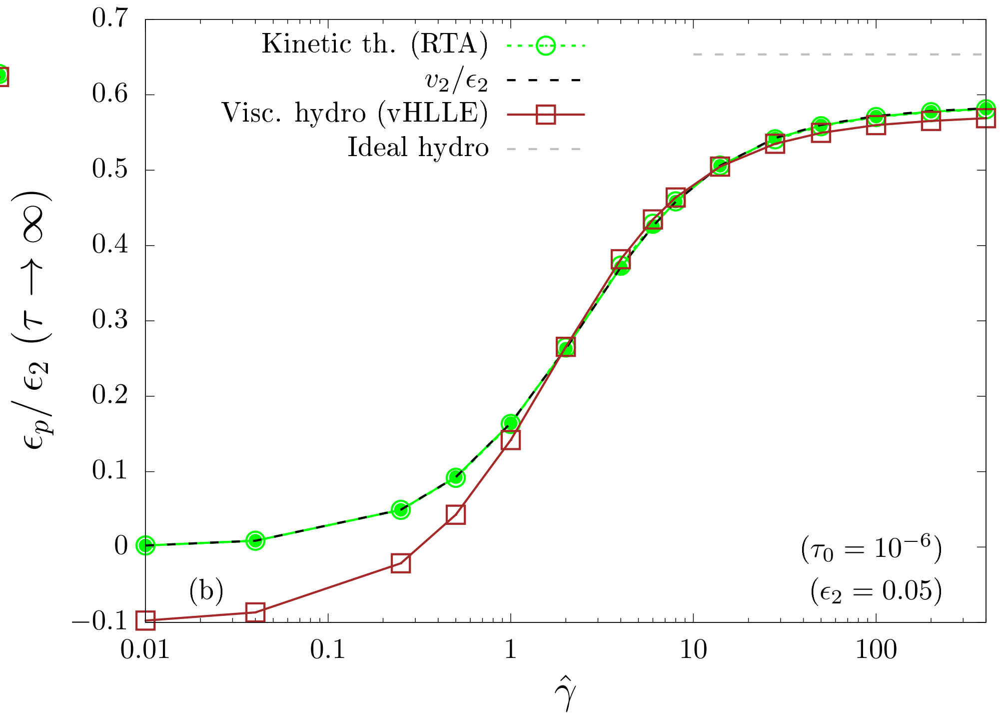

- At $\tau_0 = 0.01R$, hydro and kinetic results seem to converge at large opacities.
- At smaller $\tau_0 = 10^{-6}R$, the large opacity limits of hydro and kinetic theory do not match.

Non-commutativity of the Limits $\tau_0 \to 0$ and $\hat{\gamma} \to \infty$

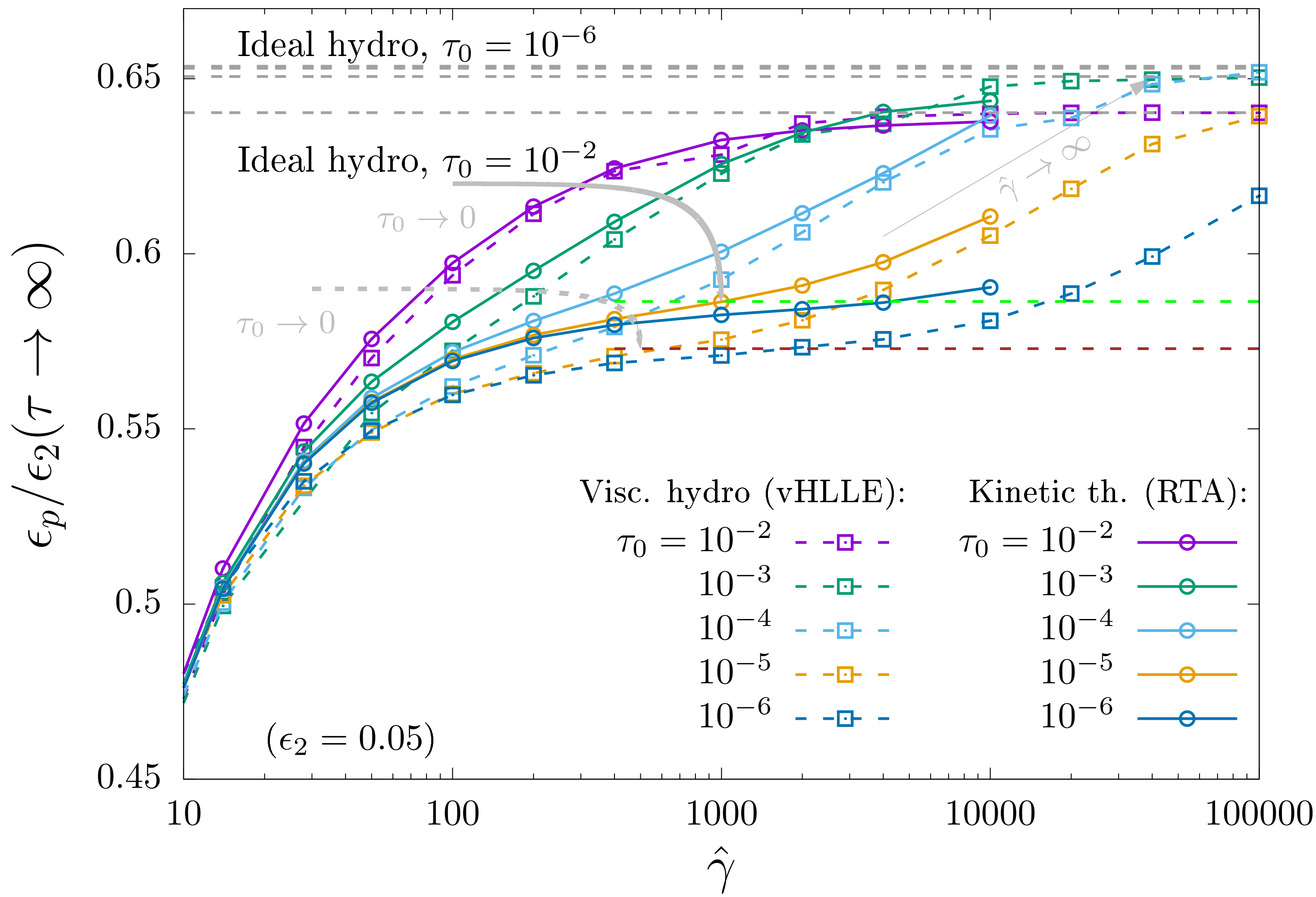

- Discrepancy from cutting out pre-equilibrium period; convergence only in unphysical order of limits ($\hat{\gamma} \to \infty$, then $\tau_0 \to 0$)
  - Need non-equilibrium description of early time dynamics even at large $\hat{\gamma}$.
- Small τ_0: curves plateau at physical large-opacity asymptote in the limit $\tau_0 \to 0$.
- Fixed τ_0: For $\tau_{eq} \lesssim \tau_0$, responses reach the (unphysical) ideal hydro limit $\hat{\gamma} \to \infty$.

(FD)RLB approach

- First, we introduce the reduced distribution $\mathcal{F}_{\rm RLB}$ via

$$\mathcal{F}_{\rm RLB} = \frac{\pi \nu_{\rm eff} R^2 \tau_0}{(2\pi)^3} \left(\frac{{\rm d}E_\perp^{(0)}}{{\rm d}\eta}\right)^{-1} \int_0^\infty {\rm d}p^\tau \, (p^\tau)^3, \tag{41}$$

such that the Boltzmann eq. becomes

$$\left(\frac{\partial}{\partial \bar\tau} + \mathbf{v}_\perp \cdot \overline{\nabla} + \frac{1+v_z^2}{\tau}\right) \mathcal{F}_{\rm RLB} - \frac{1}{\bar\tau} \frac{\partial [v_z (1-v_z^2) \mathcal{F}_{\rm RLB}]}{\partial v_z} = -\hat\gamma (v^\mu u_\mu) \overline{T} (\mathcal{F}_{\rm RLB} - \mathcal{F}^{eq}_{\rm RLB}), \tag{42}$$

with

$$\bar\tau = \frac{\tau}{\tau_0^{1/4} R^{3/4}}, \qquad \bar{\mathbf{x}}_\perp = \frac{\mathbf{x}_\perp}{\tau_0^{1/4} R^{3/4}}, \qquad \bar\epsilon = \frac{\tau_0 \pi R^2 \epsilon}{dE_\perp^{(0)}/d\eta}, \qquad \overline{T} = \left(\frac{\tau_0 \pi R^2 \frac{\pi^2}{30} \nu_{\rm eff}}{dE_\perp^{(0)}/d\eta}\right)^{1/4} T. \tag{43}$$

- Time stepping $\partial_\tau \mathcal{F}_{\rm RLB} = L[\mathcal{F}_{\rm RLB}]$ performed using RK-3 with 2 intermediate stages.
- Advection performed in an upwind-biased manner using finite differences,

$$c_1 \left(\frac{\partial \mathcal{F}}{\partial x_1}\right)_{s,r} = \frac{\mathbb{F}_{s+\frac{1}{2},r} - \mathbb{F}_{s-\frac{1}{2},r}}{\delta x_1}, \tag{44}$$

where the fluxes $\mathbb{F}_{s\pm\frac{1}{2}}$ are computed using the WENO-5 scheme.

(FD)RLB: Momentum space discretization

- $\phi_p \to \phi_{p;i} = \phi_0 + \frac{2\pi}{Q_{\phi_p}}(j - \frac{1}{2})$ [Mysovskikh trigonometric quadrature]
- $v_z \to v_{z;j} \equiv$ roots of $P_{Q_z}(v_{z;j})$ [Gauss-Legendre quadrature]
- v_z derivative can be obtained by projection onto the Legendre polynomials:

$$\mathcal{F}_{\rm RLB} = \sum_{\ell=0}^{\infty} \mathcal{F}_\ell^{\rm RLB} P_\ell(v_z) \Rightarrow \left[\frac{\partial[v_z(1-v_z^2)\mathcal{F}_{\rm RLB}]}{\partial v_z}\right] = \int_{-1}^{1} dv'_z \, \mathcal{K}_P(v_z, v'_z)\mathcal{F}(v'_z), \tag{45}$$

where

$$\mathcal{K}_P(v_z, v'_z) = \sum_{m=1}^{\infty} \frac{m(m+1)}{2} P_m(v_z) \left[\frac{m+2}{2m+3} P_{m+2}(v'_z) - \left(\frac{m}{2m-1} - \frac{m+1}{2m+3}\right) P_m(v'_z) - \frac{m-1}{2m-1} P_{m-2}(v'_z)\right]. \tag{46}$$

- After discretization, we may write

$$\left[\frac{\partial[v_z(1-v_z^2)\mathcal{F}_{\rm RLB}]}{\partial v_z}\right]_{ji} = \sum_{j'=1}^{Q_z} \mathcal{K}^P_{j,j'} \mathcal{F}^{\rm RLB}_{j'i}, \tag{47}$$

where the $Q_z \times Q_z$ matrix $\mathcal{P}_{j,j'}$ can be computed before runtime.

Small $\hat{\gamma}$: Free-streaming coordinates

- At small $\hat{\gamma}$, it is convenient to employ the following free-streaming coordinates to parametrise the momentum space:

$$\begin{aligned} p^\tau_{\rm fs} &= p^\tau \Delta, & v_z^{\rm fs} &= \frac{\tau v_z}{\tau_0 \Delta}, & \Delta &= \sqrt{1 + \left(\frac{\tau^2}{\tau_0^2} - 1\right) v_z^2}, \\ p^\tau &= p^\tau_{\rm fs} \Delta_{\rm fs}, & v_z &= \frac{\tau_0 v_z^{\rm fs}}{\tau \Delta_{\rm fs}}, & \Delta_{\rm fs} &= \sqrt{1 - \left(1 - \frac{\tau_0^2}{\tau^2}\right) v_{z;{\rm fs}}^2}. \end{aligned} \tag{48}$$

- Energy-weighted observables can be computed starting from the reduced distribution

$$\mathcal{F}_{\rm fs} = \frac{\pi \nu_{\rm eff} R^2 \tau_0}{(2\pi)^3} \left(\frac{{\rm d}E_\perp^{(0)}}{{\rm d}\eta}\right)^{-1} \int_0^\infty {\rm d}p^\tau_{\rm fs} \, (p^\tau_{\rm fs})^3 f, \tag{49}$$

which satisfies

$$\frac{\partial \mathcal{F}_{\rm fs}}{\partial \overline{\tau}} + \frac{1}{\Delta_{\rm fs}} \boldsymbol{v}_{\perp;{\rm fs}} \cdot \overline{\nabla}_\perp \mathcal{F}_{\rm fs} = -\hat{\gamma}(v^\mu u_\mu) \overline{T} (\mathcal{F}_{\rm fs} - \mathcal{F}_{\rm fs}^{eq}). \tag{50}$$

- The only change to RLB is that v_z is now discretized in logarithmic scale:

$$v_{z;j}^{\rm fs} = \frac{1}{A} \tanh \chi_j, \qquad \chi_j = \left(\frac{2j-1}{Q_z} - 1\right) {\rm arctanh} A, \tag{51}$$

where $0 < A < 1$.

- The $v_z^{\rm fs}$ integration is performed using the rectangle method:

$$\int_{-1}^1 dv_z^{\rm fs} h(v_z^{\rm fs}) \to \sum_{j=1}^{Q_z} w_j^{\rm fs} h(v_{z;j}^{\rm fs}), \qquad w_j^{\rm fs} = \frac{2 {\rm arctanh} A}{A Q_z \cosh^2 \chi_j}. \tag{52}$$

Initial conditions: Romatschke-Strickland distribution

- The system is initialized using the Romatschke-Strickland distribution for BE statistics,

$$f_{\rm RS} = \left\{ \exp\left[\frac{1}{\Lambda} \sqrt{(p\cdot u)^2 + \xi_0 (p\cdot\hat{\eta})^2} \right] - 1 \right\}^{-1}, \tag{53}$$

  where $\Lambda \equiv \Lambda(\mathbf{x}_\perp)$ satisfies

$$\Lambda^4(\mathbf{x}_\perp) = 2T^4(\tau_0, \mathbf{x}_\perp) \left(\frac{\arctan\sqrt{\xi_0}}{\sqrt{\xi_0}} + \frac{1}{1+\xi_0} \right)^{-1}, \tag{54}$$

- The anisotropy parameter ξ_0 can be used to set $\mathcal{P}_{L;0}/\mathcal{P}_{T;0}$ via

$$\frac{\mathcal{P}_{L;0}}{\mathcal{P}_{T;0}} = \frac{2}{1+\xi_0} \frac{(1+\xi_0)\frac{\arctan\sqrt{\xi_0}}{\sqrt{\xi_0}} - 1}{1 + (\xi_0 - 1)\frac{\arctan\sqrt{\xi_0}}{\sqrt{\xi_0}}}. \tag{55}$$

- $\mathcal{P}_{L;0}/\mathcal{P}_{T;0} = 0$ is achieved when $\xi_0 \to \infty$.
- For $\hat{\gamma} \geq 2$ (RLB), we used $\xi_0 = 20$ ($\mathcal{P}_L/\mathcal{P}_T =$);
- For $\hat{\gamma} \leq 2$ (FS), we used $\xi_0 = 100$ ($\mathcal{P}_L/\mathcal{P}_T =$).
- For both RLB and FS, we have

$$\mathcal{F}^{\rm RS}_{\rm RLB} = \mathcal{F}^{\rm RS}_{\rm fs} = \frac{\overline{\epsilon}/2\pi}{(1+\xi_0 v_z^2)^2} \left(\frac{\arctan\sqrt{\xi_0}}{\sqrt{\xi_0}} + \frac{1}{1+\xi_0} \right)^{-1}. \tag{56}$$

Eccentricity Dependence

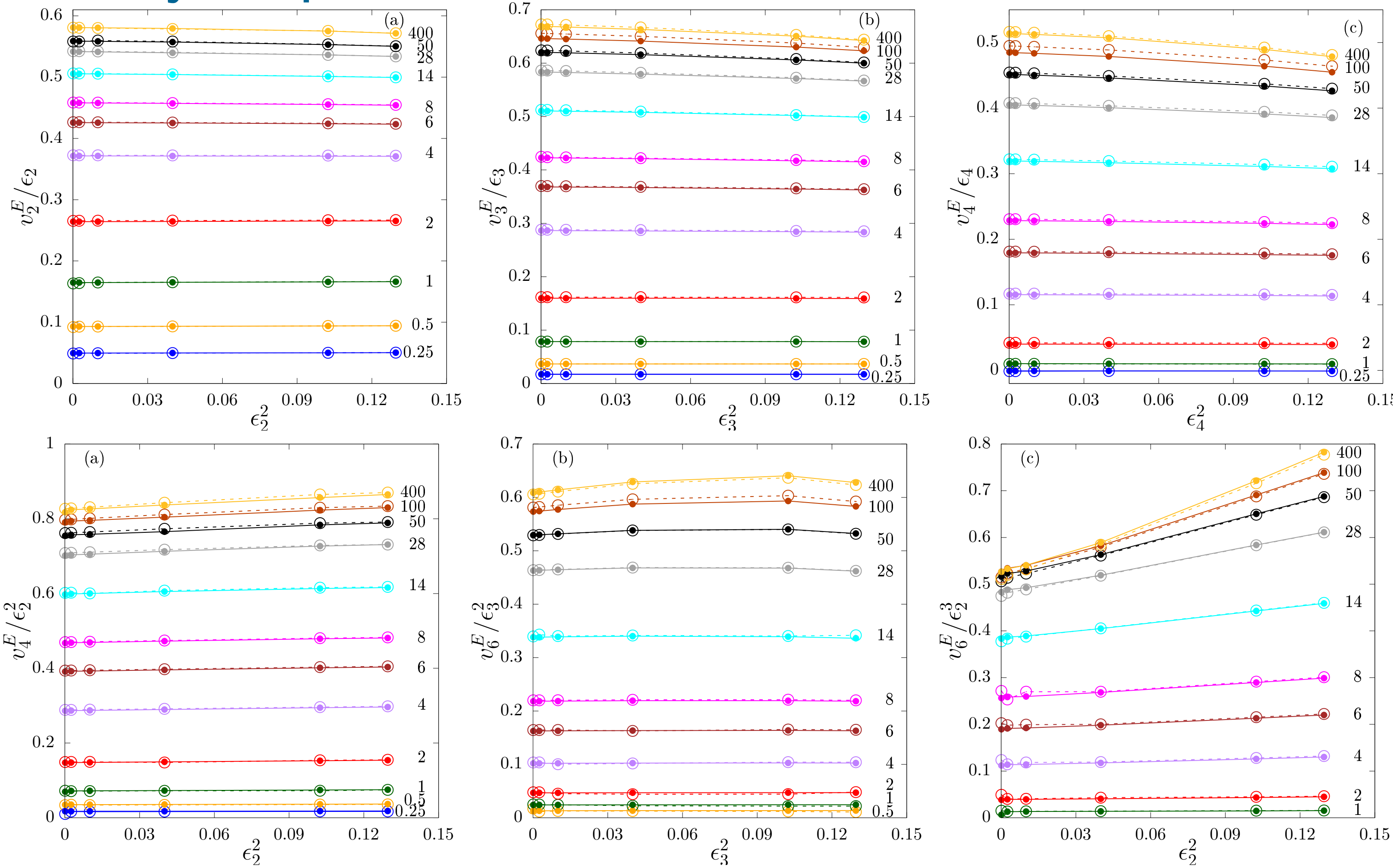

- almost no ϵ_n-dependence
- in conflict with conventional knowledge (upwards trend); even in identical setup

  Niemi, Eskola, Paatelainen PRC 93 (2016) 024907 Kurkela, Taghavi, Wiedemann, Wu PLB 811 (2020) 135901
- cross-checked this also with e.g. hydro
  - attributed to other features of specific initial state; not fully described by ϵ_n?

Eccentricity Dependence in vHLLE

$$\epsilon_p = \frac{\int_{\mathbf{x}_\perp} \left(T^{11} - T^{22} + 2iT^{12}\right)}{\int_{\mathbf{x}_\perp} \left(T^{11} + T^{22}\right)} = \frac{\int_{\mathbf{x}_\perp} \int \frac{\mathrm{d}^3 p}{(2\pi)^3}\; p^\tau \left(1 - v_z^2\right) e^{2i\phi_p}\; f}{\int_{\mathbf{x}_\perp} \int \frac{\mathrm{d}^3 p}{(2\pi)^3}\; p^\tau \left(1 - v_z^2\right) f}$$

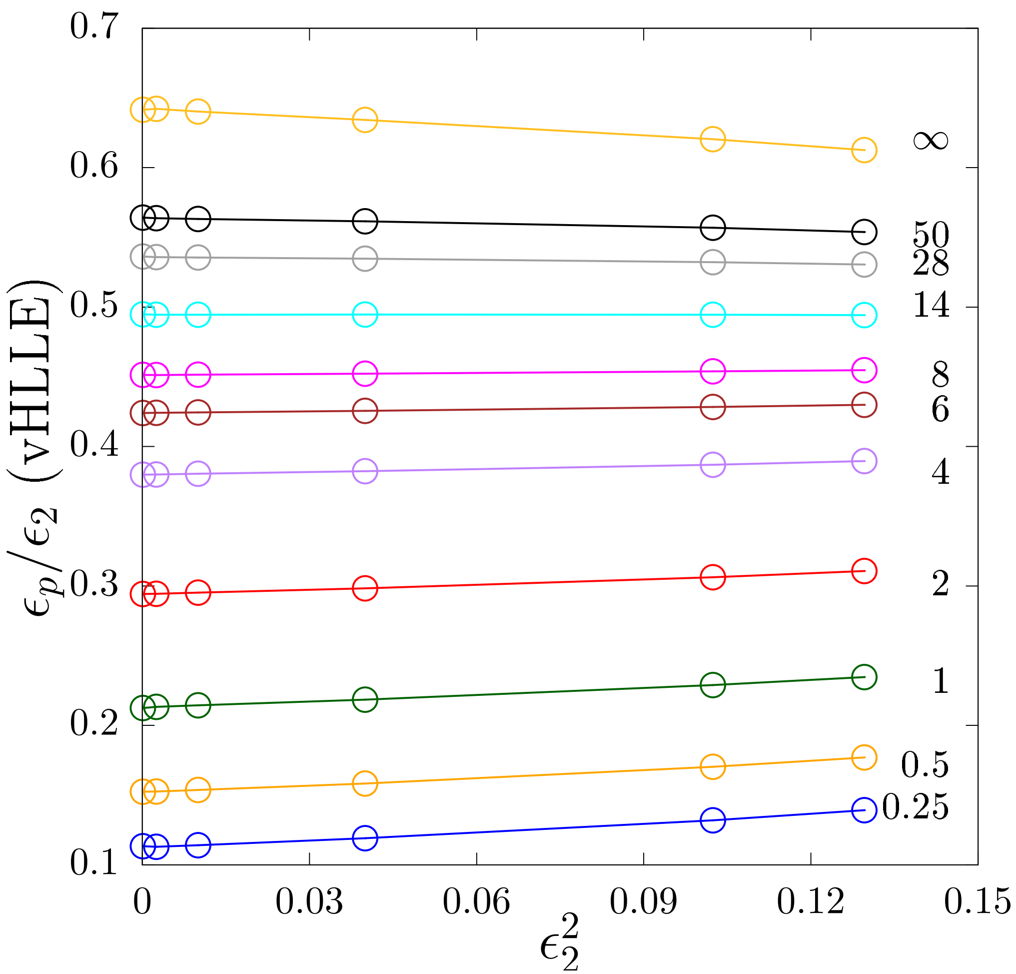

- similar to kinetic results: almost constant, negative trend at large opacities

Solutions in opacity expansion

zeroth order $p^\mu \partial_\mu f^{(0)} = 0$: $[t(\tau, \tau_0, y-\eta) = \tau\cosh(y-\eta) - \sqrt{\tau_0^2 + \tau^2\sinh^2(y-\eta)}]$

$$f^{(0)}(\tau, \mathbf{x}_\perp, \mathbf{p}_\perp, y-\eta) = f^{(0)}\left(\tau_0, \mathbf{x}_\perp - \mathbf{v}_\perp t(\tau, \tau_0, y-\eta), \mathbf{p}_\perp, \operatorname{arsinh}\left(\frac{\tau}{\tau_0}\sinh(y-\eta)\right)\right)$$

first order $p^\mu \partial_\mu f^{(1)} = C[f^{(0)}]$:

$$f^{(1)}(\tau, \mathbf{x}_\perp, \mathbf{p}_\perp, y-\eta) = \int_{\tau_0}^{\tau} \mathrm{d}\tau' \left(\frac{C[f^{(0)}]}{p^\tau}\right)(\tau', \mathbf{x}_\perp{}', \mathbf{p}_\perp, y-\eta')$$

collision kernel: find local rest frame and temperature using Landau matching to compute $C_{RTA}[f^{(0)}] = \frac{p_\mu u^\mu T}{5\,\eta/s}(f_{eq} - f)$ where $f_{eq} = [\exp(p_\mu u^\mu/T) - 1]^{-1}$

$$T^{\mu\nu} = \nu_{\text{eff}}\tau \int \frac{\mathrm{d}^3 p}{(2\pi)^3 p^\tau} p^\mu p^\nu f^{(0)} \qquad \epsilon u^\mu = u_\nu T^{\nu\mu} \qquad \epsilon = \frac{\nu_{\text{eff}}\pi^2}{30} T^4$$

free-streamed $\delta\epsilon$-cosine:

$$|\mathbf{x}_\perp - \mathbf{v}_\perp\tau|^n \cos(n\phi_{\mathbf{x}_\perp - \mathbf{v}_\perp\tau}) = \sum_{j=0}^{n} \binom{n}{j} x_\perp^{n-j}(-\tau)^j \cos[n\phi_{\mathbf{x}_\perp} + j(\phi_{\mathbf{x}_\perp} - \phi_{\mathbf{v}_\perp})]$$

Computing observables

- jacobian from milne coordinates

$$\frac{\mathrm{d}N}{\mathrm{d}^2p_\perp \mathrm{d}y}(\tau) = \nu_{\rm eff} \int \mathrm{d}^2x_\perp\, \mathrm{d}\eta\; \tau\, p^\tau\; f(\tau, \mathbf{x}_\perp, \eta, \mathbf{p}_\perp, y)$$

- extract moments relevant for flow harmonics v_n:

$$V_{mn} = \int \mathrm{d}^2p_T\; p_T^m e^{in\phi_p} \frac{\mathrm{d}N}{\mathrm{d}^2p_T \mathrm{d}y} = V_{mn}^{(0)} + V_{mn}^{(1)}, \qquad v_n^{(m)} = \frac{V_{m,n}}{V_{m,0}} = \frac{\delta V_{mn}^{(1)}}{V_{m,0}^{(0)}}$$

$$\Rightarrow V_{mn}^{(1)}(\tau) = \int_{\mathbf{p}_\perp} e^{in\phi_p}\, p_\perp^m \int_{\mathbf{x}_\perp} \int \mathrm{d}\eta \int_{\tau_0}^{\tau} \mathrm{d}\tau'\; \tau' \frac{\nu_{\rm eff}}{(2\pi)^3} \frac{p_\mu u^\mu}{\tau_R} (f_{eq} - f) \equiv V_{mn}^{(1,eq)} - V_{mn}^{(1,0)}.$$

- in total: 6d integral over $\tau', \mathbf{x}_\perp, \eta, \mathbf{p}_\perp$. 4 computed analytically, 2 numerically

$$\underbrace{V_{mn}^{(1,0)}}_{\text{decay of } f^{(0)}} = -\hat{\gamma}\delta_n V_{m0}^{(0)}\; \mathcal{P}_{mn}(\tilde{\tau}) \qquad \underbrace{V_{mn}^{(1,eq)}}_{\text{buildup of } f_{eq}} = +\hat{\gamma}\delta_n \nu_{\rm eff} R^{-m} \left(\nu_{\rm eff}^{-1} \frac{\mathrm{d}E_\perp^{(0)}}{\mathrm{d}\eta} R\right)^{\frac{m+3}{4}} \mathcal{Q}_{mn}(\tilde{\tau})$$

$$\mathcal{P}_{m0}(\tilde{\tau}) = \frac{(m+2)}{3} \int_{\tilde{\tau}_0}^{\tilde{\tau}} \mathrm{d}\tilde{\tau}' \int_0^\infty \mathrm{d}\tilde{x}_\perp\; \tilde{x}_\perp \tilde{T}\, \gamma \exp\left[-\frac{(m+2)}{3}(\Delta\tilde{\tau}'^2 + \tilde{x}_\perp^2)\right] \left[I_0\left(\frac{2m+4}{3}b\right) - \beta I_0'\left(\frac{2m+4}{3}b\right)\right]$$

$$\mathcal{Q}_m(\tilde{\tau}) = \left(\frac{\pi^2}{30}\right)^{-(m+3)/4} \frac{1}{2\pi^{1/2}}\, \Gamma(m+3)\, \zeta(m+3) \frac{\Gamma\left(\frac{m+2}{2}\right)}{\Gamma\left(\frac{m+3}{2}\right)} \int_{\tilde{\tau}_0}^{\tilde{\tau}} \mathrm{d}\tilde{\tau}' \int_0^\infty \mathrm{d}\tilde{x}_\perp\; \tilde{x}_\perp \tilde{\tau}'\, \tilde{T}^{m+4} \gamma^{-m-2}$$

$$\times\; {}_2F_1\left(\frac{m+2}{2}, \frac{m+2}{2}; 1; \beta^2\right)$$